Nanoparticles of Alkylglyceryl-Dextran-*graft*-Poly(Lactic Acid) for Drug Delivery to the Brain: Preparation and In-Vitro Investigation

Petr Toman[1], Chun-Fu Lien[1], Zeeshan Ahmad[2], Suzanne Dietrich[1], James R. Smith[1], Qian An[1], Éva Molnár[1], Geoffrey J. Pilkington[1], Darek C. Górecki[1], John Tsibouklis[1], Eugen Barbu[1]*

1. School of Pharmacy and Biomedical Sciences, University of Portsmouth, St Michael's Building, White Swan Road, Portsmouth, PO1 2DT, United Kingdom

2. Leicester School of Pharmacy, De Montfort University, Leicester, LE1 9BH, United Kingdom

* eugen.barbu@port.ac.uk

Abstract

Poly(lactic acid), which has an inherent tendency to form colloidal systems of low polydispersity, and alkylglyceryl-modified dextran – a material designed to combine the non-immunogenic and stabilising properties of dextran with the demonstrated permeation enhancing ability of alkylglycerols – have been combined for the development of nanoparticulate, blood brain barrier-permeating, non-viral vectors. To this end, dextran, that had been functionalised *via* treatment with epoxide precursors of alkylglycerol, was covalently linked to poly(lactic acid) using a carbodiimide cross-linker to form alkylglyceryl-modified dextran-*graft*-poly(lactic acid). Solvent displacement and electrospray methods allowed the formulation of these materials into nanoparticles having a unimodal size distribution profile of about 100 - 200 nm and good stability at physiologically relevant pH (7.4). The nanoparticles were characterised in terms of hydrodynamic size (by Dynamic Light Scattering and Nanoparticle Tracking Analysis), morphology (by Scanning Electron Microscopy and Atomic Force Microscopy) and zeta potential, and their toxicity was evaluated using MTT and Presto Blue assays. Cellular uptake was evidenced by confocal microscopy employing nanoparticles that had been loaded with the easy-to-detect Rhodamine B fluorescent marker. Transwell-model experiments employing mouse (bEnd3) and human (hCMEC/D3) brain endothelial cells revealed enhanced permeation (statistically significant for hCMEC/D3) of the fluorescent markers in the presence of the nanoparticles. Results of studies using Electric Cell Substrate

Impedance Sensing suggested a transient decrease of the barrier function in an *in vitro* blood-brain barrier model following incubation with these nanoformulations. An *in ovo* study using 3-day chicken embryos indicated the absence of whole-organism acute toxicity effects. The collective *in vitro* data suggest that these alkylglyceryl-modified dextran-*graft*-poly(lactic acid) nanoparticles are promising candidates for *in vivo* evaluations that would test their capability to transport therapeutic actives to the brain.

Keywords: nanoparticles, drug delivery, butylglyceryl dextran, poly(lactic acid), alkylglycerols, blood-brain barrier, endothelial cells, cytotoxicity.

Introduction

The extent of neurodegenerative, cerebrovascular, inflammatory, neoplastic and infectious brain diseases is expected to rise with increasing average life expectancy and with the current advances in diagnostic methods.[1] In treating brain ailments, the intravascular route appears attractive compared to other approaches due to the proximity of the brain parenchymal cells to brain capillaries and the large surface area of the brain vessel network.[2] Transport from the blood-stream into the brain however is generally limited by the presence of the blood-brain barrier (BBB), which has an important role in maintaining the specific environment required for neuronal signalling. The presence of tight junctions and efflux proteins, together with processes such as selective abluminal transport and the flow of intracerebral fluid, act additively to restrict entry into the brain of toxins, xenobiotics and molecules endogenous to the circulatory system that may otherwise compromise the homeostasis of the neuronal environment.[3]

Among several approaches aimed at overcoming the BBB (including osmotic opening, prodrugs, intracerebral implants, convection-enhanced delivery or focused ultrasound), colloidal systems such as nanoparticles or liposomes are now widely accepted as an effective tool for transporting essential actives into the brain. Although studies in this very active area of research have shown that these carriers may take advantage of the biochemical transport systems present at the barrier level, the mechanism of BBB transport is still under debate.[4-11]

Poly(lactic acid) (PLA) is commonly used for various tissue engineering and drug delivery applications not only due to its biodegradability, biocompatibility and to being non-immunoactive, but also due to its capacity to form colloidal systems of low polydispersity.[12,13] While the hydrophobicity of pure PLA nanoparticles normally leads to a rapid removal from the bloodstream by the reticulo-endothelial system upon *iv* injection,[14] this shortcoming may be addressed by

modification with hydrophilic materials of natural origin, such as dextran.[15-17] Considered non-toxic and non-immunogenic, dextran has been used historically as a safe plasma expander[18] and also to impart stabilisation in the blood-stream and "stealth" properties to injectable nanoparticles.[19,20] Among the materials investigated for enhancing drug penetration across the BBB, alkylglycerols have been shown to encourage a strong but transient increase in the transport of actives into the brain.[21-24] If co-administered into the right internal carotid artery, the same materials have been found to increase brain uptake of certain antineoplastic agents (such as cisplatin and methotrexate) or antibiotics (such as vancomycin and gentamycin) in C6 glioma bearing rats and animals with RG2 implanted tumours.[25,26]

Rationalised by the hypothesis that the assemblage of a drug-carrier system based on dextran that had been modified with alkylglyceryl moieties and the easily biodegradable poly(lactic acid) could promote increased drug permeability towards the brain, we report on the formulation and physicochemical characterisation of nanoparticulate non-viral vectors prepared from alkylglyceryl-dextrans and poly(acrylic acid) and assess their toxicity and permeability/interaction with *in vitro* models of the BBB based on mouse and human brain capillary endothelial cells (bEnd3 and hCMEC/D3).

Experimental

General. Dextran from Leuconostoc (MW 6 kDa), dimethyl sulfoxide (DMSO, anhydrous, ≥ 99.9 %), butyloxymethyloxirane (OX4, 95 %), 4-(dimethylamino) pyridine (DMAP, puriss. > 99 %), $Zn(BF_4)_2$, potassium tert-butoxide (t-BuOK; reagent grade > 97 %), carbonyldiimidazole (CDI, reagent grade), toluene (anhydrous, 99.8 %) were all obtained from Sigma Aldrich, Gillingham, UK. Poly(lactic acid) (PLA) with free carboxyl group (PLA-02A, MW 15 kDa) was a gift from Purac, Gorinchem, Netherlands. Fast green, Paraformaldehyde, Evans Blue and Rhodamine B were purchased from Sigma Aldrich, Gillingham, UK; Doxorubicin hydrochloride was obtained from LGM Pharma, Nashville, USA; non-anhydrous solvents were obtained from Fisher Scientific, Loughborough, UK; high purity deionised water was sourced from a PURELAB Optima lab system. Gentamycin was supplied from Gibco, Paisley, UK; fountain ink (India) was purchased from Pelikan. Unless otherwise specified, all reagents were used as obtained. Dulbecco's Modified Eagle Medium (DMEM) media, TrypLE Express™, Hoechst Blue 33342, Phosphate Buffered Saline (PBS), and PrestoBlue assay were purchased from Invitrogen Life Technologies, Paisley, UK. Matrigel was sourced from BD Biosciences, Plymouth, UK. EGM-2 Bullet Kit™ (containing Endothelial Growth Medium with SingleQuots™: growth factors, cytokines and supplements) was purchased from Lonza, Slough, UK. Recovery™ Cell Culture Freezing Medium, Hank's Balanced

Saline Solution (HBSS), and distilled water (cell culture quality) were purchased from Gibco, Paisley, UK. Trypan blue, Fluorescein Isothiocyanate (FITC) labelled dextran, and L-cysteine were purchased from Sigma Aldrich, Gillingham, UK. Cryo-vials Greiner bio-one and sterile Nunc 96 well-plates were obtained from Fisher Scientific, Loughborough , UK. MTT Cell Proliferation Assay Kit and digitonin were sourced from Invitrogen Life Technologies, Paisley, UK. Sterile Transwell 24 well-plates were obtained from Millipore, Livingstone, UK (Millicell-24 Cell Culture Plate; polyethylene terephthalate membrane; 1.0 µm; filtration surface 0.33 cm^2; pore density 2×10^6 cm^{-2}); 8-well 8WE10 array Electric Cell Substrate Impedance Sensing (ECIS) plates were sourced from Applied Biophysics, New York, USA.

Thin Layer Chromatography silica gel plates F254 were obtained from Merck, London, UK. Dialysis was performed using Visking membrane tubing (Medicell International Ltd, London, UK) with cut-off either at 12-14 kDa or at 3 kDa, in a discontinuous system (10.0 L deionised water, exchanged 3 times/day). Cellulose nitrate membrane filters (0.2 µm) were obtained from Whatman, Maidstone, UK.

Solvent removal under reduced pressure was performed using a Büchi Rotovapor R-200 powered with a Sogevac Saskia PIZ 100 vacuum pump equipped with a liquid nitrogen trap. Solvents were degassed using three freeze-thawing cycles. Sonication was performed using a Grant ultrasonic bath XB3 (Farnell, UK). Low speed centrifugation was performed using a Jouan B4i centrifuge equipped with a S40 rotor (4 000 rpm; 2 880 g; 15 min, unless otherwise specified). Ultracentrifugation was performed using a X3 Ultracentrifuge (Beckman Coulter Ltd. UK) with Ti 70.1 rotor at 20 °C *in vacuo* (40 000 rpm; 164 391 *g*; 30 min), and pre-centrifugation was performed with an Eppendorf MiniSpin centrifuge equipped with a F-45-12-11 rotor (Eppendorf UK). Freeze drying of aqueous samples (flash frozen using liquid nitrogen) was performed using an Edwards Micro Modulyo Freeze Dryer equipment (-50 °C) attached to an EDWARDS RV3 vacuum pump (4×10^{-2} mbar). Sonication was performed using a Grant ultrasonic bath XB3 from Farnell, UK. A high voltage power supply (PSIFC30R04.0-22; Glassman High Voltage Inc, USA) was employed for electrospraying experiments, in combination with a syringe pump Alladin 300 (World Precision Instruments, USA). A combined linear shaking water bath with thermostat (Grant OLS 200, Farnell, UK) was used for dye-release studies. A pumping device (Pneumatic PicoPump pv820, World Precision Instruments, USA) was used for *in ovo* intracardial administration *via* a glass micro-needle. A Vibratome Series 1000 (Section Vibratome System) was used for microscopy sample preparations, which were visualised using a confocal microscope (LSM 710, ZEISS, Germany).

Materials were characterised by ^{1}H- and ^{13}C-NMR spectroscopy using a JEOL Eclipse 400+ instrument (Jeol, UK; 400 MHz for ^{1}H- and 100 MHz for ^{13}C-NMR); samples were dissolved in either $CDCl_3$, D_2O or DMSO-d_6 employing 0.2 % TMS as a reference, and spectra were processed using the JEOL Delta v 5.0.2 software. FT-IR spectra were recorded using a Nicolet 6700 instrument (Thermo Scientific, UK) equipped with an ATR Smart Orbit™ accessory with diamond crystal, at 128 scans and 4 cm^{-1} resolution. FTIR spectral analysis was performed using Omnic Specta 8.0 software. Characterisation data is presented as Supplementary Material. A Lambda 650 Ultra Violet/Visible Spectrometer from Perkin Elmer was used for UV/VIS spectroscopy measurements (Perkin Elmer UV Lab software). Statistical analysis was performed using OriginPro 7 software from OriginLab, USA by one-way analysis of variance (ANOVA) followed by Tukey test and Bonferroni-corrected post hoc T-test (p values were set at level 0.05, unless stated otherwise). Data are presented as mean ± standard deviation.

Synthesis of alkylglycerol-dextran derivatives (DEX-O4 and DEX-OX 8). The synthesis of n-alkyloxymethyloxiranes (OX-4 and OX-8) was carried out according to a method described previously.[27] Dextran (1.00 g; 6.10 mmol) was dissolved in anhydrous DMSO (200 mL). The base (potassium tert-butoxide, either 1.36 g (12.20 mmol) or 2.72 g (22.40 mmol); or pyridine 0.96 g (12.20 mmol); or DMAP 1.49 g (12.20 mmol)) was dissolved in anhydrous THF (50 mL) and added dropwise into the DMSO solution of Dextran. The mixture was allowed to stir for 2 h before the dropwise addition of a solution of oxirane (OX4: 63 mmol, 9.0 mL, d=0.91; or OX8: 63 mmol, 12.6 mL) in DMSO (20.0 mL). The reaction mixture was stirred for 48 h at room temperature (25 °C) then dialysed extensively (MWCO 3 kDa) against deionised water (10.0 L; exchanged 3 × per day) for three days. The content of the dialysing membrane (approx. 400 mL) was washed with diethylether (3 × 150 mL) in a separation funnel, to remove water-insoluble impurities. After removing the traces of volatile solvents in a rotary evaporator under reduced pressure (25°C), the aqueous layer was lyophilised affording alkylglyceryl-modified dextrans (butylglyceryldextran DEX-OX4 and octylglyceryldextran DEX-OX8) as a slightly brown powder. Yields were in range 52-73 %. The final products were characterised with FTIR, ^{1}H - and ^{13}C – NMR spectroscopy.

Synthesis of alkylglyceryl dextran-graft-poly(lactic acid) derivatives (PLA-DEX-OX4 and PLA DEX-OX8) was carried out by a modification of Nagahama's procedure.[16] In a reaction apparatus that was degassed and purged with nitrogen, poly(lactic acid) (PLA, 0.50 g, 0.033 mmol) in anhydrous chloroform (7.0 mL) was added drop-wise to a solution of carbodiimidazole (CDI, 0.11 g, 0.66 mmol) in anhydrous chloroform (5.0 mL). The reaction mixture was stirred for 6 h at room temperature under nitrogen, and then washed with ethanol (10 mL) to remove the excess CDI and

imidazole. The resultant precipitate was collected by centrifugation and dried overnight *in vacuo* (25 °C). The presence of the imidazoyl group in the CDI-activated PLA (yield 82-90%), obtained as white crystalline powder, was confirmed by ^{1}H-NMR spectroscopy. In the second step alkylglyceryl-dextran (DEX-OX4 0.20 g, 0.66 mmol, DEX-OX8, 0.24 g, 0.66 mmol) and 4-(dimethylamino)pyridine (DMAP, 0.08 g, 0.60 mmol) were each dissolved in anhydrous DMSO (50 mL); CDI-activated PLA (0.40 g, 0.027 mmol) was dissolved in anhydrous DMSO (50 mL) and added drop-wise to the DEX-OX & DMAP solution. The reaction mixture was stirred at room temperature for 24 h under nitrogen, after which time the reaction was stopped by adding conc. HCl (150 μL) to neutralise any DMAP and imidazole. The reaction mixture was dialysed against deionised water for 48 h then freeze-dried. The solid residue was washed thoroughly with acetone to remove excess PLA and with water to remove unreacted alkylglyceryl-dextran. The purified products (yields 68-81%) were freeze-dried and characterised by FT-IR, ^{1}H- and ^{13}C-NMR spectroscopy.

Preparation of nanoparticles by solvent displacement. A solution of PLA-DEX-OX4 (either 0.5, 1.0, 3.0, or 5.0 mg/mL) in DMSO (10.0 mL) was filtered through a 0.2 μm filter (PP membrane) and then dialysed (MWCO 12 000 Da) against deionised water for 72 h (10.0 L; exchanged 3 times per day) to remove the DMSO. For PLA-DEX and PLA-DEX-OX8 nanoparticles were prepared using a concentration of 1.0 mg/mL. After 48 h, the content of the dialysing tubing was freeze-dried and the solid material was redispersed as nanoparticles in PBS (0.9 % NaCl; pH 7.4) or in ultrapure water (conductivity 18 MΩ; pH 7.0). The suspension was centrifuged at low speed (3 000 rpm; 603 *g*; 5 min, Eppendorf MiniSpin) to remove any potential large aggregates formed, and then the nanoparticles were analysed by Dynamic Light Scattering (DLS), Nanoparticle Tracking Analysis (NTA) and Electrophoretic Mobility Measurements (EPM).

Preparation of nanoparticles by electrospraying. Nanoparticles from PLA-DEX-OX4 were prepared using a single-needle electrospray setup. A solution (1.0 mL) of PLA-DEX-OX4 in DMSO (5 % w/v) was infused using a syringe pump (Alladin 300; World Precision Instruments, USA) into a needle which was connected to the high-voltage generator (PSIFC30R04.0-22; Glassman High Voltage Inc) and the sprayed material was collected onto a water surface (50 mL water, contained in a circular dish, surface area 143.1 cm^{2}). The purification of the resulting dispersion was performed either *via* ultracentrifugation (Beckman, Rotor 70.1 Ti; 40 000 rpm; 164 391 *g*; 30 min; 20 °C) or *via* dialysis (for 3 days, 10.0 L of deionised water exchanged 3 x per day) and freeze-drying. The nanoparticles were then redispersed in ultrapure water or PBS (pH 7.4; 0.9 % saline) and the

suspension was centrifuged at low speed (3 000 rpm; 603 *g*; 3 min) to remove any potential aggregates prior to being analysed by DLS, EPM and NTA.

Physical characterisation of nanoparticles. A Malvern Zetasizer Nano ZS instrument equipped with a 633 nm He-Ne laser (173° back-scattering angle detection) and controlled by Zetasizer v6.01 software was used to determine the hydrodynamic diameter of nanoparticles; samples were analysed at 25 °C in triplicate using clear polycarbonate disposable cuvettes and following an equilibration time of 2 min. Results of cumulative analysis were expressed as Z-average mean (Z-av) and the polydispersity index (PDI) was also reported. Zeta potential was determined from electrophoretic mobility measurements (EPM) using the same instrument; for this purpose, samples were measured in folded capillary cells (DTS1070, Malvern) and data was processed according to Smoluchowski's model (Henry's function $f(ka)$ = 1.5)). A MTP-2 (Multi-Purpose Titrator-2, Malvern, UK) equipped with a solvent degasser was employed to investigate pH dependency. Samples (10 mL each) were titrated automatically with aqueous NaOH solutions (5 mM and 50 mM) from pH 3 to pH 8, and with aqueous HCl solutions (5 and 50 mM) from pH 8 to pH 2; all solutions were filtered *via* 0.2 μm PES filters (Whatman) prior to use.
Nanoparticle Tracking Analysis (NTA) was performed at 25 °C using a Nanosight instrument with a thermostatted LM-14 unit equipped with a 532 nm green laser and controlled by the NTA v2.2 analytical software; the image capture (60 s) was achieved using a CCD Marlin camera.

The nanoparticle morphology was investigated by Scanning Electron Microscopy (SEM) and Atomic Force Microscopy (AFM). Samples were prepared by redispersion of nanoparticles in ultrapure water and placing a droplet (5 μL) onto mica adhered onto an aluminium stub (SEM) or adhered onto a nickel disk (AFM) for 2 min, followed by drying in a nitrogen flow. Samples for SEM were sputter-coated with Au/Pd (Ar atmosphere; 20 mA, 10^{-3} Pa, 5 min; Quorum coater Q150RES, Quorum Technologies Ltd., UK) and then investigated using a JEOL-JSM-6060LV SEM Microscope (voltage 15 kV, working distance 11 mm, spot size 40). For AFM investigations a MultiMode/NanoScope IV Scanning Probe Microscope (Digital Instruments, USA) was employed in tapping mode, in air, under ambient conditions (T = 23 °C, RH = 21%). A J-scanner (max. xy = 170 μm) and Si cantilevers with integrated tips (t = 3.5–4.5 μm, l = 115–135 mm, w = 30–40 μm, f_0 = 200–400 kHz, k = 20–80 N m^{-1}, R < 10 nm; Model: RTESP, Bruker, France) and an RMS amplitude of 0.8 V were used. The results were analysed using Nanoscope v 710 software (Bruker).

Loading and release studies using fluorescent drug / markers. Fluorescein isothiocyanate (FITC), Rhodamine B and Doxorubicin free base were loaded following the same methods as for the preparation of nanoparticles (namely solvent displacement and electrospraying, as described above). Rhodamine B and Doxorubicin free base were dissolved in DMSO (10 % w/w in respect to the polymer); Doxorubicin free base was obtained from commercial hydrochloride salt by treatment with triethylamine followed by extraction with dichloromethane. Drug loading was determined by UV-Vis spectroscopy following separation of nanoparticles by ultracentrifugation (40 000 rpm; 164 391 g; 30 min, 20°C, Beckman, rotor 70.1 Ti); pellets were freeze-dried, measured for mass and dissolved in DMSO to determine the amount of dye by UV/Vis (measuring at 318 nm for Rhodamine B; 493 nm for FITC; 478 nm for Doxorubicin), and the results were plotted against calibration curves of the same fluorescent molecules obtained in DMSO.

For release studies, the freeze-dried PLA-DEX-OX4 nanoparticles were redispersed (at a concentration of 1.0 mg/mL) in PBS (15 mL, pH 7.4, saline 0.9 %) and transferred into Eppendorf tubes (1.0 mL each) that were then incubated at 37 °C in a shaker / water bath with thermostat. Tubes were then individually removed at pre-determined time points and centrifuged (13 000 rpm; 11 336 *g*; 15 min; Eppendorf MiniSpin); three aliquots (0.1 mL each) were removed from the supernatant and placed into a 96 well-plate which was kept in the freezer (-20 °C) until all samples were collected, the plate was then equilibrated at 25 °C and subsequently analysed using an Optima fluorimeter. The release profiles of dyes in PBS were then calculated using calibration curves of the corresponding fluorescent molecules dissolved in PBS.

In vitro cell cultures. bEnd3 immortalised mouse brain endothelial cells were obtained from the Health Protection Agency Culture Collections UK and hCMEC/D3 immortalised (hTERT/SV40) human brain endothelial cell cells were a kind gift of Pierre-Olivier Couraud from Institut Cochin, INSERM, Paris, France . Cells were cultured under humidified atmosphere (hCMEC/D3 in a standard Mini Galaxy E incubator, bEnd3 in a Nuaire DH AUTOFLOW Air-Jacketed incubator) at 37 °C and 5 % CO_2 in small T25 culturing (Fisher) flasks. Details of the culturing media are presented in Table S2 (Supplementary material). Nunclon F 96-well plates were sourced from Thermo Scientific. Cells were observed with an Olympus IX71 inverted phase microscope (images were taken using Olympus Soft Imaging System, UK) and with an LSM 710 confocal microscope (Zeiss, fluorescence excitation at 405 nm, 488 nm and 633 nm; facilitated by a Twin Gate main beam splitter). Cells were counted using either a Vi-CELL XR Cell Viability Analyser (Beckman Coulter, UK) or a haemocytometer. The analysis of well-plates was performed using a POLARstar Optima

(BMG Labtech) plate-reader. Electric Cell-substrate Impedance Sensing (ECIS) measurements were conducted with an ECIS Zθ instrument (Applied Biophysics) operating at a frequency range of 2 - 32 kHz and using 8 well-arrays type 8W10E.

Cytotoxicity assays. Nanoparticles (formulated from PLA-DEX; PLA-DEX-OX4 and PLA-DEX-OX8) were tested for cytotoxicity against bEnd3 cells (seeding 1×10^4 cells,) using an MTT assay. Nanoparticles were suspended in modified DMEM (1 mg/mL) and used to incubate with confluent bEnd3 cells (24 h). Sterile PBS (without nanoparticles) and Digitonin (1 % w/v in PBS) were used as negative and positive control, respectively (details as Supplementary material). A PrestoBlue assay was employed to assess the dose-dependent cytotoxicity of the same nanoformulations (0.2 – 4.0 mg/mL) against hCMEC/D3 cells (seeding 1×10^4 cells) at different time points (3 h and 24 h); PBS and Digitonin were similarly employed as negative and positive controls (details as Supplementary material).

In-ovo toxicity investigations. Embryos in their early stage of development (embryos in Hamburger-Hamilton HH stage 19, day 2; eggs supplied from a local farm after fertilisation and stored prior use at 15 °C in a cold storing room) were employed for these studies. Eggs (n = 6) were placed into an incubator (37 °C, 60-70 % humidity) 48 h prior to nanoformulation treatment. After 72 h in the incubator, a needle was inserted through the eggshell at the narrow apex to remove the excess of egg white. Adhesive tape was used to cover the egg on the top (to prevent the structure from collapsing) and a small oval window was cut into the shell, through the tape. 100 µL of gentamycin in PBS (10 % w/v) was instilled inside the egg as an antibiotic pre-treatment prior to any manipulation. Fountain pen ink was then injected under the embryo to provide a contrast background for easier orientation and manipulation. The vitelline membrane enveloping the embryo was then cut with a forceps to reach the heart area. A thin glass micro-needle (diameter 25 µm) connected to a pneumatic pumping device was used to inject the nanoformulation into the heart of the embryo, close to aorta. Rhodamine B-loaded PLA-DEX-OX4 nanoformulations (5 µL; 1 mg/mL; Rhodamine loading 1.5 % w/w, by electrospraying) were employed for this study, with a Rhodamine B solution (5 µL; 0.015 mg/mL) used as a control.
A Fast Green solution (1 % v/v, 1 µL) was added to the nanoformulations prior to injection to allow visualising the spread of nanoparticles through the blood stream of the embryos. The egg cavity was instilled again with a dose of the antibiotic (as above), and the shell window was sealed with transparent adhesive tape. The eggs were then further incubated (37 °C, 60-70 % humidity) for 24 h before harvesting the embryos. The embryos were removed from the eggs and cleaned by removing

the rest of the vitelline membrane (by forceps), fixed for 15 min in paraformaldehyde solution in PBS (4 % w/v), and embedded in hot gelatine (60 °C). After storing for 2 h at 4 °C, the embryos were removed and sectioned using a vibratome (50 μm slices). The analysis was performed by a confocal microscope (using a 543 nm laser to visualise Rhodamine B).

Cell uptake studies. bEnd3 cells were seeded (5.0×10^4) onto glass cover slips previously coated with Matrigel 1.5 mg/mL and incubated for 24 h in 2.0 mL of modified DMEM (composition given in Table S2, Supplementary material) in a 6 well plate. Media was then replaced with 2.0 mL of each nanoformulation (2 mg of PLA-DEX-OX4 nanoparticles loaded with Rhodamine B (0.5 % w/w) dispersed in 2 mL of DMEM) and the cover slips were further incubated for 3 h. As control, cells were incubated in Rhodamine B solution of the same concentration as that of the Rhodamine present in the nanoformulation, namely 2.0 mL of cell media containing 0.001 mg of Rhodamine B base (prepared from stock solution, 1 mg/mL); a blank control was provided by incubating cells in DMEM without any addition of nanoparticles or dye. After incubation, cells were washed twice with PBS, fixed for 10 min in paraformaldehyde (4.0 % w/v) at 4 °C, permeabilised for 20 min with Triton X-100 (0.1 % v/v), and incubated for 40 min with nuclear counter-stain Hoechst 33342 (5.0 μg/mL) at 25 °C. The cells were then visualised using a confocal microscope (LSM 710, Zeiss, 405 nm for Hoechst, 543 nm for Rhodamine B).

Nanoparticle-induced FITC translocation studies. Nanoparticles prepared from PLA-DEX-OX4 were investigated for their effect on the cellular transport of FITC-labelled dextran (FITC-DEX, MW 150 kDa) across confluent endothelial cell monolayers using a Transwell-type BBB model. 24 well plates Millipore Millicell (PET membrane; 1 μm pore diameter; 600 μL max volume) were washed twice with Hank's Balanced Saline Solution (HBSS;500 μL) and equilibrated with water for 15 min at 37 °C. The filter membranes were then coated with ice-cold Matrigel (150 μL; 1.5 mg/mL) and incubated for 15-30 min at 37 °C to promote better cell adhesion. After coating, filters were washed twice with HBSS and either mouse or human brain endothelial cells were seeded (3×10^5 bEnd3 cells per well; 2×10^5 hCMEC/D3 cells per well). Plates were incubated at 37 °C in corresponding media (details in Table 2S, Supplementary material), which was replaced every 2 days in both apical and receiving compartments. As a control, cells were also seeded in a standard 24 well plate to monitor their health and confluence (as the opacity of the Transwell filter did not allow for microscopy-based cell inspection). The experiments were carried out after reaching cell confluence, usually 3-4 days from seeding. In case of bEnd3 cells, a specific cocktail of barrier enhancers (consisting of 250 μM cAMP, 20 μM RO-20-1724, and 550 μM hydrocortisone) was applied after

24 h of cells reaching confluence. Nanoformulations containing PLA-DEX-OX4 nanoparticles in the concentration range 1-4 mg/mL (or PLA-DEX, 4 mg/mL, as control), dispersed in the corresponding media, were added to each well together with fluorescently-labelled dextran (FITC-DEX, 100 μg/mL), and the concentration of FITC-DEX in the receiving compartment was then monitored over time by sampling (100 μL) at 30 min intervals from the receiving compartment and replacing the volume removed with fresh media. Samples (triplicate) were collected into 96-well plates and analysed using a fluorescence plate reader Optima BMG (excitation 485 nm; emission 520 nm). The concentration of FITC-DEX was determined using a calibration curve of FITC-DEX in cell media) and was further used to calculate the apparent permeability coefficient (P_{app}), as described by Arthursson:[28]

$$P_{app}(cm.s^{-1}) = \frac{dQ}{dt} \times \frac{V_R}{A \times C_0 \times 60} \qquad (1)$$

where:

d*Q*/d*t*	the flux of FITC-DEX transported across the membrane (μg/s);
V_R	basolateral volume (600 μL);
A	surface area of the filter insert (0.33 cm^2);
C_0	initial mass concentration of FITC-DEX at the apical side (100 μg/mL)
60	conversion factor (min to s)

Electric Cell-Substrate Impedance Sensing (ECIS) studies. Polycarbonate 8 well arrays (Applied Biophysics, USA; 8W10E) were employed; the wells were washed twice with HBSS and equilibrated with cell culture grade water. The electrodes were stabilised by incubation with L-cysteine (10 mM) for 15 min at 25 °C. The plates were washed again with HBSS and coated with Matrigel 1.5 mg/mL (incubation at 37 °C for 15 min), then washed again briefly with HBSS prior to seeding cells (either hCMEC/D3; 2.5×10^5 cells per well, or bEnd3; 3×10^5 cells per well; one well was left empty as control), and the plate was incubated at 37 °C. After reaching confluence (40-50 h, indicated by a plateau in resistance over time: ~ 1500 Ω for hCMEC/D3, and ~ 800 Ω for bEnd3 cells), the media was replaced with a mix of fresh media (350 μl) and PBS-based nanoformulation (50 μl of PBS containing dispersed nanoparticles in a concentration range 1 – 4 mg/mL for PLA-DEX-OX4, and 4 mg/mL PLA-DEX). After incubation with nanoparticles (24 h), the nanoformulation was removed and replaced with fresh media, and well were further monitored for 24 h. ECIS readings were taken continuously for the whole duration of the experiment using an ECIS Zθ instrument (Applied Biophysics, USA) at 2 000 Hz.

Results and discussion

Dextrans were modified by grafting with alkylglyceryl chains (where alkyl was either butyl, pentyl, or octyl) *via* a nucleophilic substitution reaction with the corresponding alkyloxy-substituted oxirane in an alkaline environment; this was followed by coupling with poly(lactic acid) using carbodiimide chemistry to afford alkylglyceryl-dextran-*graft*-poly(lactic acid), Figure 1.

Figure 1

The degree of substitution with alkylglyceryl chains (defined as the number of pendent chains per 100 glucopyranose rings of dextran) was found to be directly dependent on the strength of the base and on the excess of oxirane employed. Various bases (pyridine, DMAP and t-BuOK) were tested: while pyridine's basicity was not sufficient and DMAP yielded only low degrees of substitution (2.1-6.6 %), best results (up to 75% degree of substitution) were obtained with t-BuOK at 48 h reaction time and 4 times molar excess of oxirane. Attempts to employ $Zn(BF_4)_2$ as a catalyst in acidic aqueous media (pH 1, as reported in the literature for similar reactions)[29,30] only resulted in products with a low degree of substitution (< 1.8 %). Following product purification by extraction and dialysis, the modification of dextran with alkyl glyceryl chains was confirmed by FT-IR and ^{1}H- / ^{13}C-NMR spectroscopy. Introduction of alkylglyceryl chains resulted in the formation of new secondary alcohol and ether groups, evidenced by changes in the fingerprint region (such as the 1127 cm^{-1} band, C–O–C; 1343 cm^{-1}, O–C–H; 1539 cm^{-1} CH_2 group vibration); in the ^{1}H-NMR spectra of alkylglyceryl-modified dextran, the resonances at 0.86 ppm (3 H; CH_3), 1.29 ppm (2 H, CH_2) and 1.45 ppm (2 H, CH_2) are indicative of the presence of the alkylglyceryl modification. The signal of the anomeric proton (C1; 4.67 ppm) was well separated from the signals of the other protons of the glucopyranosyl ring (3.2–3.7 ppm), in agreement with data for similar structures reported in the literature;[31] the multiplet at 4.96 ppm was assigned to the protons from the hydroxyl groups of dextran.

The degree of substitution (expressed as number of alkylglyceryl chains per 100 glucopyranose units; DS%) was calculated from ^{1}H-NMR spectra using Equation 2:

$$DS[\%] = \frac{\frac{1}{3} \times \int C4\prime}{\int C1} \times 100 \qquad (2)$$

where C4' is the integral of the signal assigned to the alkyl chain CH_3 end group (0.86 ppm; Figure 1), and C1 is the integral of the signal assigned to the anomeric proton from of the glucopyranose ring (4.67 ppm).

The degree of substitution varied widely (from 0.7 to 75.1 % for DEX-OX4, and from 16.5 to 38.2 % for DEX-OX8), and it was found to increase with reaction time and with the concentration of base (*t*-BuOK) employed. Since the calculated degree of substitution never exceeded 100 %, and considering that the OH group reactivity in dextran towards alkylation agents is known to decrease in the order C2 > C4 > C3 (likely due to the proximity to the anomeric C1 carbon),[32-35] it can be reasonably assumed that only the primary hydroxy groups were grafted with alkylglyceryl chains.

Poly(lactic acid) with free carboxylic end group was attached to the alkylglyceryl-modified dextran using carbodiimide chemistry, with either N,N'-dicyclohexylcarbodiimide (DCC) or N,N'-carbonyldiimidazole (CDI). Following purification by repeated washings with water and acetone to remove potentially un-reacted PLA, final products were obtained after freeze-frying as off-white powders. Higher yields were obtained with CDI (68-81 %) than with DCC (33-56 %). Strong IR bands at 1751 cm^{-1} and 3352 cm^{-1} characteristic of the C=O stretching vibration in PLA and of the OH stretching vibrations of the dextran backbone confirmed the success of the grafting process, as did the ^{1}H-NMR spectra, which exhibited characteristic bands for butylglyceryl-modified dextran (0.87 ppm; CH_3 of alkylglyceryl chain; 3.22-5.14 ppm glucopyranose ring) and for poly(lactic acid) (1.44 ppm, CH_3; 5.19 ppm, CH). A conjugate of poly(lactic acid) and unmodified dextran (PLA-DEX) was prepared using CDI and used as control. The ratio between PLA and modified dextran enumerated the degree of grafting (DG; defined as the number of PLA polymeric units per 100 glucopyranose units of dextran), which was calculated from ^{1}H-NMR spectra using Equation 3 below,

$$DG = \frac{\frac{1}{3}\int a}{\int C1} \times 100 \qquad (3)$$

where: a integral of the signal attributed to the CH_3 group in PLA (1.31 ppm)

C1 integral of the signal attributed to the anomeric proton of dextran (4.39 - 5.17)

The degree of grafting was found to decrease slightly with increasing length of the alkylglyceryl chain used for the hydrophobic modification of dextran: PLA-DEX (130-142 %); PLA-DEX-OX4 (108-120 %); PLA-DEX-OX8 (88-112 %).

The size range of nanoparticles prepared from PLA-DEX-OX4 by solvent displacement was found to be consistent with those reported in the literature for poly(lactic acid) dextran copolymers.[16,36] The same parameter was found to be dependent on the concentration of polymer in the DMSO solution that had been subjected to dialysis (Figure 2A), with concentrations below 6 mg/mL affording the

smallest particle size (diameter 120 - 160 nm). Also, no significant statistical difference was found in the size of nanoparticles obtained from different PLA-conjugated modified dextran polymers (PLA-DEX, PLA-DEX-OX4, PLA-DEX-OX8) using the solvent displacement formulation method at the concentration of 1.0 mg/mL (Figure 2B).

Figure 2

Further experiments employing electrospraying techniques where PLA-DEX-OX4 solutions in DMSO (50 mg/mL) were subjected to high voltage electric field resulted in the formation of particles at the 100 - 200 nm diameter range. As with nanoprecipitation, this technique requires post-purification of nanoparticles either by dialysis or ultra-centrifugation. A comparison of the characteristics measured for the PLA-DEX-OX4 nanoparticles formulated using different methods (Table 1) suggests that size (as measured in PBS saline 0.9 %, at pH 7.4, by both DLS and NTA) is in all cases suitable for intravascular drug delivery at physiological pH, [37] with the solvent displacement method offering the advantage of higher yields.

Table 1

The pH stability of PLA-DEX-OX4 nanoformulations was investigated by titrating nanoparticles dispersed in ultrapure water while monitoring their size and zeta potential, which at pH 7.4 was in the range -15 to -30 mV for all formulations. Both average size and zeta potential were stable over a wide range of pH values (2 - 8), however an increase in size and a gradual agglomeration were noticed near the isoelectric point of poly(lactic acid), as expected from its pK_a value (3.1) (Figure 3).

Figure 3

Investigations of the morphology of freeze-dried PLA-DEX-OX4 nanoparticles prepared by dialysis indicated a spherical shape (Figure 4) and submicron size diameter (PLA-DEX-OX4 - horizontal 64.4 ± 11.7 nm, vertical 15.4 ± 2.2 nm); PLA-DEX - horizontal 52.5 ± 15.4 nm, vertical 14.4 ± 4.5 nm; as measured by AFM). The difference between the vertical and horizontal dimensions of AFM images are attributed to the deformation induced by the pressure exerted by the tip on the probed nanoparticle. The aggregates observed in the SEM micrograph are assumed to have been formed during the evaporation of liquid media at the sample preparation stage. The differences observed when comparing these results with those obtained for the same type of nanoparticles in colloidal

form are likely due to the hydration of the outer layer and also possibly due to an induced conformational change of polymer chains at the surface of nanoparticles.[38]

Figure 4

Doxorubicin free base, Fluorescein isothiocyanate (FITC), and Rhodamine B free base were employed as drug models and fluorescence markers respectively. The molecules were selected due to their low detection limits and limited photobleaching. They were loaded into PLA-DEX-OX4 nanoparticles prepared by either solvent displacement or by electrospraying, and drug/marker loading was determined by fluorescence measurements; results (Table 2) clearly indicate that electrospraying provides a more efficient loading method compared to solvent displacement. FITC was found to load poorly into PLA-DEX-OX4 nanoparticles and to be released under simulated physiological conditions with a burst effect that was complete within 30 min (Figure 5). In contrast, Rhodamine B and Doxorubicin (both as free base) showed better loading and gradual release 30 to 50 % over several hours.

Table 2

Figure 5

Despite recent drug-delivery advances that seem to hold great promise for the treatment of CNS diseases, very little is known about the long-term safety of nanomaterials employed in these studies, therefore testing the toxicity of these nanoformulations in early stages of development is of importance. We found that incubation of mouse brain endothelial cells bEnd3 with poly(lactic acid)-*graft*-alkylglyceryldextran (PLA-DEX-OXn) nanoparticles (1 mg/mL) for 24 h revealed no significant toxicity induced by these nanoformulations (ANOVA $p < 0.05$); cell viability following treatment with PLA-DEX, PLA-DEX-OX4 and PLA-DEX-OX8 nanoparticles was about 90 % of that of a PBS control (Figure 6A). Experiments with human brain endothelial cells (hCMEC/D3) at different concentrations confirmed the lack of toxicity at short incubation times (3 h) and appeared to suggest that the alkylglyceryl modification of dextran shows a higher viability compared to PLA-DEX (Figure 6B); however, incubation for 24 h revealed a gradual reduction in viability at doses higher than 2 mg/mL (ANOVA, $p < 0.05$) (Figure 6C).

Figure 6

Figure 7

Injections into the heart of chicken embryos with nanoformulations prepared from PLA-DEX-OX4 and loaded with Rhodamine B showed that nanoparticles did not aggregate in circulation and did not affect the viability of the embryos; 100 % viability (n = 6) was observed for both control and nanoparticles (as evidenced by the heart function of the embryos) for the duration of the experiment (min. 24 h following injections). No specific patterns were observed in the biodistribution of the fluorescent marker, which appeared to extravasate freely into the embryo as all the endothelial barriers including the BBB are still leaky at this development stage.[39] Most of the fluorescence appeared around blood vessels, and no significant differences were observed in the distribution of Rhodamine B between the two administration methods employed (i.e. as solution, or loaded into nanoparticles and later released during incubation; Figure 7).

Nanoparticles prepared from PLA-DEX-OX4 were loaded with Rhodamine B (0.5 % w/w) and investigated for their interactions with bEnd3 cells after 3 h incubation in DMEM. Confocal microscopy indicated that Rhodamine B-loaded carriers were taken up by the bEnd3 cells as evidenced by the presence of the fluorescent dye in the cytoplasm and in the peri-nuclear space (Figure 8); there was no similar evidence of the Rhodamine B being inside cells that was used as a control solution. While there was no evidence of targeting the nuclei, the nanoparticles appeared to have been localised in vesicles (possibly Golgi apparatus, as previously demonstrated for CS-OX4 nanoparticles).[21]

Figure 8

The effect of PLA-DEX and PLA-DEX-OX4 nanoformulations on the integrity of confluent endothelial cell monolayers was investigated by monitoring changes in the transendothelial resistance (TEER) of either mouse bEnd3 or human hCMEC/D3 cell monolayers, both during incubation and following removal of nanoparticles. The mouse model reached ~ 800 Ω resistance while the human model exhibited a resistance of ~1500 Ω when the cell cultures achieved confluence (*ca.* 48 h). Results of TEER measurements for a range of concentrations (1 to 4 mg/ml) - presented as values relative to the PBS control, Figure 9 - indicated differences in the behaviour of mouse brain endothelial bEnd3 cells that had been treated with PLA-DEX nanoparticles as compared with those treated with PLA-DEX-OX4 nanoparticles; a drop in TEER values was observed for all concentrations of the latter. To assess the capability of cells to recover following nanoparticle-induced stress, TEER was monitored for longer periods of time than those found in complementary experiments to be readily tolerated by the cells (Figure 6B). The data in Figure 9 indicate that at high concentrations (4 mg/ml) there is a non-reversible drop in TEER after 72 h, which may be attributed

to cell death (as supported by the decrease in cell viability observed at high nanoparticle concentrations, Figure 6C). Following nanoparticle removal, TEER levels recovered for all monolayers except those that had been treated with the highest dose of PLA-DEX-OX4 (significant statistical difference for bEnd3 cells at 72 h, ANOVA, $p < 0.05$, Figure 9A); this may be attributed to the time- and concentration-dependent toxicity of PLA-DEX-OX4 nanoparticles. No significant dose-response effect could be unmasked when the formulation was tested against human-brain endothelial hCMEC/D3 cells (Figure 9B).

Figure 9

Investigations of the capability of PLA-DEX-OX4 nanoparticles to increase drug permeability through mouse and human brain endothelial cell monolayers were carried out using a translocation model system based on a Transwell setup, where the effect of each nanoformulation was assessed using fluorescent FITC-labelled dextran (MW 150 kDa). In a comparison of the two types of models, data suggested that the bEnd3 model was more permeable than that based on hCMEC/D3 cells (Figure 10); the latter may therefore be more suitable for this type of permeability experiments as it also could reveal the concentration-dependent effect induced by PLA-DEX-OX4 nanoparticles (statistically significant for hCMEC/D3 cells at 4 mg/mL dose, compared with controls; ANOVA $p < 0.05$).

Figure 10

Translocation studies utilised the concentration of fluorescently labelled dextran (FITC-dextran) present in the apical compartment of the Transwell system as the indicator of the permeation enhancing properties of nanoparticles under investigation. The apparent permeation coefficient (P_{app}), calculated from the concentration of FITC-dextran transported across a unit surface area of the barrier over a specified timescale, corresponds to the translocating capacity of a cellular monolayer of a population of the cell culture.[28] As determined from the amount of translocated FITC-DEX, the data presented in Table 3 suggest that over a 3 h incubation time PLA-DEX-OX4 nanoparticles at high doses are more effective at modulating the permeability of hCMEC/D3 cell monolayers as compared with PLA-DEX nanoparticles. Since toxicity experiments have demonstrated that at relatively short incubation times the alkylglyceryl modification is not associated with any additional toxicity effects to cells (Figure 6B), the increased transport of FITC-DEX cannot be readily attributed to cell death (and the consequent development of "leaky holes" in the monolayers); increased cytotoxicity is however noticeable with high doses (4 mg/ml) at long incubation times (> 72 h). While PLA-DEX nanoparticles were seen to increase the transport of

FITC-DEX to some extent (possibly *via* non-specific nanoparticle-cell interaction),[40] data appear to support the hypothesis that the alkylglyceryl modification could possibly increase barrier permeability *via* mediated opening of the tight junctions. This is further supported by data from ECIS experiments, which revealed transient drops in TEER values upon the application of nanoparticles.

Table 3

Lower P_{app} values were obtained for the hCMEC/D3 cell model than for that employing bEnd3 cells (Table 3), which indicates the better barrier properties of the human brain cells model. While our P_{app} values obtained with the mouse cell model were consistent with literature values (1×10^{-7} at 4 h of incubation),[41] those for the human cell model are different.[42,43] This may be explained in terms of the modifications in experimental protocol or may be consequent to the introduction of non-physiologically relevant features into the system.[44,45] Irrespective of the reason for this difference, our results indicate that the use of a barrier enhancing formulation to decrease the permeability of the cell monolayers is effective.

Conclusions

Alkylglyceryl-modified dextran-*graft*-poly(lactic acid) derivatives (PLA-DEX-OXn; prepared by the alkylglycerol functionalisation of dextran and its subsequent attachment to the terminal carboxylic group of poly(lactic acid) by means of carbodiimide cross-linkers) can be easily formulated into nanoparticles that appear to be good candidates for drug delivery or for imaging applications. Nanoparticles of average size in the 100-200 nm range exhibited unimodal size distribution profiles, as determined by DLS and NTA, and a negative zeta potential, as evidenced by electrophoretic mobility measurements. Formulations of these nanoparticles exhibit good stability at around neutral pH. The relative uniformity of nanoparticle size has been confirmed in the solid state by the SEM and AFM imaging of freeze dried samples. These nanoparticles may be prepared using any of three techniques (solvent displacement, nanoprecipitation or electrospraying) and are amenable to loading with actives or with fluorescent markers; the electrospraying technique has been identified as particularly useful for the loading of Doxorubicin.

In general, nanoformulations displayed low toxicity against mouse bEnd3 and human hCMEC/D3 brain endothelial cells, even at relatively high doses (80 % viability for 2 mg/mL, after 24 h incubation). However, over prolonged incubation times (> 72 h), doses of nanoparticles at the 4 mg/ml level appeared to negatively affect the cell monolayers integrity. As assessed by investigations involving early development-stage chicken embryos, PLA-DEX-OX4 nanoparticles did not exhibit any propensity to aggregation in blood circulation. Alkylglyceryl functionalisation

has been shown to impact little upon the toxicity of nanoparticles, as assessed by comparative studies involving their unmodified congeners at similar concentrations.

Microscopy investigations using bEnd3 mouse brain endothelial cells have indicated the cellular uptake of Rhodamine B-labelled butylglyceryl modified nanoparticles PLA-DEX-OX4 and their tendency to agglomerate at the perinuclear region. TEER measurements on monolayers of bEnd3 or hCMEC/D3 brain endothelial cells have demonstrated the capability of nanoformulations to induce concentration-dependent transient changes to monolayer integrity.

The *in vitro* permeability of fluorescent FITC dextran through hCMEC/D3 brain endothelial cell monolayers has been seen to increase on co-administration with butylglyceryl modified nanoparticles PLA-DEX-OX4, suggesting the enhanced cellular transport of the tracer; administration of non-modified nanoparticles PLA-DEX at the same concentration did not induce a similar effect.

The collective *in vitro* data suggest that these alkylglyceryl-modified dextran-poly(lactic acid) nanoparticles are promising candidates for *in vivo* evaluations of their capability to transport therapeutic actives or fluorescent markers into the brain.

We acknowledge the financial assistance from the Institute of Biological and Biomedical Sciences (IBBS), University of Portsmouth (PhD stipend for PT) and we thank Dr. P.O. Couraud (INSERM, Paris) for the hCMEC/D3 cells; GP and ZA also acknowledge British Tumour Research and the Royal Society for their partial support.

Tables

Table 1 . Characteristics of nanoparticles prepared from PLA-DEX-OX4 using different techniques (n = 3).

Table 2. Loading of fluorescent molecules into PLA-DEX-OX4 nanoparticles using different techniques (n = 3, ±SD).

Table 3a. Apparent permeability coefficients (P_{app}) for PLA-DEX and PLA-DEX-OX4 nanoparticles measured in human and mouse brain endothelial cell models (3 h incubation time; FITC-DEX as control; n=6, ±SD).

Table 3b. Statistical significance of apparent permeability coefficients (P_{app}); p values indicate significance if < 0.005 (Bonferroni-corrected post hoc T-test).

Table 1. Characteristics of nanoparticles prepared from PLA-DEX-OX4 (a) and PLA-DEX (b) using different techniques (n = 3).

Formulation technique	Diameter NTA nm ±SD		Diameter DLS nm ±SD		PDI (DLS)		Zeta Potential mV ±SD	Yields PLA-DEX-OX4 (%; after purification) ±SD	
	(a)	(b)	(a)	(b)	(a)	(b)		Dialysis	Centrifugation
Solvent displacement (1 mg/mL)	123 ±85	113 ±23	161 ±61	132 ±63	0.18 ±0.03	0.12 ±0.09	-22 ±7	71 ±19	13 ±5*
Nanoprecipitation (5 mg/mL)	142 ±53	104 ±15	152 ±48	150 ±37	0.15 ±0.05	0.12 ±0.07	-23 ±7	44 ±23	15 ±7
Electrospraying (50 mg/mL)	155 ±63	136 ±12	143 ±69	141 ±51	0.12 ±0.03	0.17 ±0.09	-25 ±8	61±16	20 ±13

* n = 2

Table 2. Loading of fluorescent molecules into PLA-DEX-OX4 nanoparticles using different techniques (n = 3, ±SD).

	Drug loading (% mass)	
	Solvent displacement	Electrospraying
FITC	0.02 ± 0.01	-*
Rhodamine B	0.32 ± 0.11	4.93 ± 0.76
Doxorubicin	0.50 ± 0.23	12.57 ± 3.17

* not measured (could not be loaded)

Table 3a. Apparent permeability coefficients (P_{app}) for PLA-DEX and PLA-DEX-OX4 nanoparticles measured in human (hCMEC/D3) and mouse (bEnd3) brain endothelial cell models (3 h incubation time; FITC-DEX as control; n=6, ±SD).

P_{app}±SD [cm s^{-1}] at 3 h	FITC-DEX 150 kDa	PLA-DEX-OX4 1 mg/mL	PLA-DEX-OX4 2 mg/mL	PLA-DEX-OX4 4 mg/mL	PLA-DEX 4 mg/mL
bEnd3	(1.36±0.24) × 10^{-7}	(1.52±0.81) × 10^{-7}	(1.70±0.51) × 10^{-7}	(1.70±0.39) × 10^{-7}	(1.63±0.41) × 10^{-7}
hCMEC/D3	(1.38±0.22) × 10^{-8}	(1.22±0.09) × 10^{-8}	(1.95±0.03) × 10^{-8}	(2.41±0.13) × 10^{-8}	(1.41±0.06) × 10^{-8}

Table 3b. Statistical significance of apparent permeability coefficients (P_{app}); p values indicate significance if < 0.005 (Bonferroni-corrected post hoc T-test).

p values (T-test)		FITC-DEX 150 kDa	PLA-DEX-OX4 1 mg/mL	PLA-DEX-OX4 2 mg/mL	PLA-DEX-OX4 4 mg/mL	PLA-DEX 4 mg/mL
bEnd3	FITC-DEX 150 kDa	-				
	PLA-DEX-OX4 1 mg/mL	0.656735031	-			
	PLA-DEX-OX4 2 mg/mL	0.169592255	0.651089519	-		
	PLA-DEX-OX4 4 mg/mL	0.095557895	0.631365511	0.996752012	-	
	PLA-DEX 4 mg/mL	0.197481850	0.776992499	0.785540214	0.754566273	-
hCMEC/D3	FITC-DEX 150 kDa	-				
	PLA-DEX-OX4 1 mg/mL	0.134252930	-			
	PLA-DEX-OX4 2 mg/mL	0.000099116	0.000000005	-		
	PLA-DEX-OX4 4 mg/mL	0.000002102	0.000000006	0.000010315	-	
	PLA-DEX 4 mg/mL	0.724262400	0.001501892	0.000000004	0.000000014	-

Figure legends

Figure 1. Generic structure of alkylglyceryl-dextran-graft-poly(lactic acid) co-polymers.

Figure 2. A) The effect of polymer concentration on the hydrodynamic diameter of nanoparticles formulated from PLA-DEX-OX4 via solvent displacement; B) Hydrodynamic diameter of nanoparticles formulated by the same method from DMSO solution (1 mg/mL) of different types of PLA-dextran conjugate materials. Error bars represent ±SD (n=3).

Figure 3. Variation of PLA-DEX-OX4 nanoparticles characteristics (size and zeta potential) with decreasing pH (1 mg/mL dispersion prepared by solvent displacement, adjusted with NaOH 0.05 M to pH 8, and then titrated with HCl 0.05 M and 0.005 M using a MPT-2 Malvern Autotitrator (n = 3; error bars represent ±SD).

Figure 4. SEM (left) and AFM images (right) of freeze-dried PLA-DEX-OX4 nanoparticles prepared via solvent displacement.

Figure 5. Release profiles from loaded PLA-DEX-OX4 nanoparticles (1 mg/ml) in PBS (pH 7.4; saline 0.9 %) at 37 °C for: A) FITC; B) Rhodamine B; C) Doxorubicin (n=3, ±SD).

Figure 6. Results of toxicity studies following incubation of different types of brain endothelial cells with nanoparticles formulated from poly(lactic acid)-graft-alkylglyceryldextran derivatives ((PLA-DEX-OX4 - poly(lactic acid)-graft-alkylglyceryldextran, PLA-DEX-OX8 - poly(lactic acid)-graft-butylglyceryldextran, PLA-DEX - poly(lactic acid)-graft-dextran), at different incubation times and using different types of cytotoxicity assays (PBS and, digitonin as controls; error bars represent standard deviation): A) bEnd3 cells incubated with 1 mg/mL of nanoparticles for 24 h; MTT assay (n=18, ±SD); B) hCMEC/D3 cells incubated with nanoparticles for 3 h, dose response, PrestoBlue assay (n=12, ±SD); C) hCMEC/D3 cells incubated with PLA-DEX-OX4 nanoparticles for 24 h, dose response (1 – 4 mg/mL); PrestoBlue assay (n=12, ±SD).

Figure 7. Confocal microscopy images (a - fluorescence 543 nm; b - differential interference contrast (Nomarski); c – merged; 100 μm scale bar) of somite microtome sections following injection in chicken embryos with: 1) nanoparticles loaded with Rhodamine B (1.5 % w/w)*; 2)*

Rhodamine B solution of equivalent dose. Image 3) shows an illustration of somites (adapted from ref.[46]) and the site of our injections (1 mm scale bar).

Figure 8. Confocal microscope images of bEnd3 cells following incubation with PLA-DEX-OX4 nanoparticles (1 mg/mL) for 3 h (1 a-c), with Rhodamine B solution (equivalent concentration of dye) used as control (2 a-c): a) images of cell nuclei, Hoechst-counterstained, in blue (405 nm laser); b) images of Rhodamine B label, in red (543 nm laser), c) merged images (405 nm and 543 nm lasers); 50 μm scale bars. Image (3) is a three dimensional Z stack projection of optical sections of bEnd3 cells containing PLA-DEX-OX4 nanoparticles loaded with Rhodamine B (20 μm scale bar).

Figure 9. Electric Cell-substrate Impedance Sensing (ECIS) plot of the variation of TEER values (as %, relative to control) at 2000 Hz using A) bEnd3 and B) hCMEC/D3 brain endothelial cell monolayers cultured on 8W10E test plates, following exposure to and then removal of nanoparticles(timepoints indicated by orange arrows) prepared from PLA-DEX and PLA-DEX-OX4, in dose-response experiments. Nanoformulations were added to the cells at 48 h and removed at 72 h, after which the cells were allowed to recover for a further 48 h. Data presented as means of three wells (n = 3), for each condition of a representative measurement (error bars represent ±SE). Untreated cells (PBS, no nanoparticles added) were employed as control.

Figure 10. The effect of nanoformulations on the FITC-dextran (150 KDa) translocation through brain endothelial cell layers, at different concentrations: A) mouse bEnd3 cells model; B) human hCMEC/D3 cells model. Nanoparticles were prepared from PLA-DEX-OX4, and from PLA-DEX; FITC-dextran was used as a control (n = 5, ±SD).

References

(1) Olesen J, Gustavsson A, Svensson M, Wittchen HU, Jönsson B; CDBE2010 study group; European Brain Council. The economic cost of brain disorders in Europe. Eur J Neurol. 2012;19:155-162.

(2) Pardridge WM. Drug Targeting to the Brain. Pharm Res. 2007;24:1733-1744.

(3) Omidi Y, Barar J. Impacts of blood-brain barrier in drug delivery and targeting of brain tumors. BioImpacts. 2012;2:5-22.

(4) Kreuter J. Nanoparticulate systems for brain delivery of drugs. Adv Drug Deliv Rev. 2012;64:213-22.

(5) Wohlfart S, Khalansky AS, Gelperina S, Begley D, Kreuter J. Kinetics of transport of doxorubicin bound to nanoparticles across the blood-brain barrier. J Control Release. 2011;154:103-107.

(6) Trapani A, De Giglio E, Cafagna D, Denora N, Agrimi G, Cassano T, Gaetani S, Cuomo V, Trapani G. Characterization and evaluation of chitosan nanoparticles for dopamine brain delivery. Int J Pharm. 2011;419:296-307.

(7) Frank RT, Aboody KS, Najbauer J. Strategies for enhancing antibody delivery to the brain. Biochim Biophys Acta. 2011;1816:191-198.

(8) Barbu E, Molnàr E, Tsibouklis J, Górecki DC. The potential for nanoparticle-based drug delivery to the brain: overcoming the blood-brain barrier. Expert Opin Drug Deliv. 2009;6:553-565.

(9) Kreuter J, Gelperina S. Use of nanoparticles for cerebral cancer. Tumori. 2008;94:271-277.

(10) Alyautdin R, Khalin I, Nafeeza MI, Haron MH, Kuznetsov D. Nanoscale drug delivery systems and the blood-brain barrier. International Journal of Nanomedicine. 2014;9(1):795-811.

(11) Nicolas J, Mura S, Brambilla D, MacKiewicz N, Couvreur P. Design, functionalization strategies and biomedical applications of targeted biodegradable/biocompatible polymer-based nanocarriers for drug delivery. Chem Soc Rev. 2013;42(3):1147-235.

(12) Charles-Harris M, del Valle S, Hentges E, Bleuet P, Lacroix D, Planell JA. Mechanical and structural characterisation of completely degradable polylactic acid/calcium phosphate glass scaffolds. Biomaterials. 2007;28:4429-4438.

(13) Romero-Cano MS, Vincent B. Controlled release of 4-nitroanisole from poly(lactic acid) nanoparticles. J Control Release. 2002;82:127-135.

(14) Verrecchia T, Spelnehauer G, Basile DV, Murry-Brelier A, Archimbaud Y, Veillard M. Non-stealth (poly(lactic acid/albumin)) and stealth (poly(lactic acid-polyethylene glycol)) nanoparticles as injectable drug carriers. J Control Release. 1995;36:49-61.

(15) Cadée JA, van Luyn MJ, Brouwer LA, Plantinga JA, van Wachem PB, de Groot CJ, den Otter W, Hennink WE. In vivo biocompatibility of dextran-based hydrogels. J Biomed Mater Res. 2000;50:397-404.

(16) Nagahama K, Mori Y, Ohya Y, Ouchi T. Biodegradable nanogel formation of polylactide-grafted dextran copolymer in dilute aqueous solution and enhancement of its stability by stereocomplexation. Biomacromolecules. 2007;8:2135-2141.

(17) Zhao Z, Zhang Z, Chen L, Cao Y, He C, Chen X. Biodegradable stereocomplex micelles based on dextran-block-polylactide as efficient drug deliveries. Langmuir. 2013;29:13072-13080.

(18) McCahon R, Hardman J. Pharmacology of plasma expanders. Anaesth Intensive Care Med. 2007;8:79-81.

(19) Easo SL, Mohanan PV. Dextran stabilized iron oxide nanoparticles: Synthesis, characterization and in vitro studies. Carbohydr Polym. 2013;92(1):726-32.

(20) Jaulin N, Appel M, Passirani C, Barratt G, Labarre D. Reduction of the uptake by a macrophagic cell line of nanoparticles bearing heparin or dextran covalently bound to poly(methyl methacrylate). J Drug Target. 2000;8(3):165-72.

(21) Marigny K, Pedrono F, Martin-Chouly CA, Youmine H, Saiag B, Legrand AB. Modulation of endothelial permeability by 1-O-alkylglycerols. Acta Physiol Scand. 2002;176:263-268.

(22) Erdlenbruch B, Alipour M, Fricker G, Miller DS, Kugler W, Eibl H, Lakomek M. Alkylglycerol opening of the blood-brain barrier to small and large fluorescence markers in normal and C6 glioma-bearing rats and isolated rat brain capillaries. Br J Pharmacol. 2003;140:1201-1210.

(23) Hülper P, Veszelka S, Walter FR, Wolburg H, Fallier-Becker P, Piontek J, Blasig IE, Lakomek M, Kugler W, Deli MA. Acute effects of short-chain alkylglycerols on blood-brain barrier properties of cultured brain endothelial cells. Br J Pharmacol. 2013;169:1561-1573.

(24) Erdlenbruch B, Schinkhof C, Kugler W, Heinemann DE, Herms J, Eibl H, Lakomek M. Intracarotid administration of short-chain alkylglycerols for increased delivery of methotrexate to the rat brain. Br J Pharmacol. 2003;139:685-694.

(25) Erdlenbruch B, Jendrossek V, Kugler W, Eibl H, Lakomek M. Increased delivery of erucylphosphocholine to C6 gliomas by chemical opening of the blood-brain barrier using intracarotidal pentylglycerols in rats. Cancer Chemother Pharmacol. 2002;50:299-304.

(26) Erdlenbruch B, Jendrossek V, Eibl H, Lakomek M. Transient and controllable opening of the blood-brain barrier to cytostatic and antibiotic agents by alkylglycerols in rats. Exp Brain Res. 2000;135:417-422.

(27) Molnár E, Barbu E, Lien CF, Górecki DC, Tsibouklis J. Toward drug delivery into the brain: synthesis, characterization, and preliminary in vitro assessment of alkylglyceryl-functionalized chitosan nanoparticles. *Biomacromolecules.* 2010;11:2880-2889.

(28) Artursson P. Epithelial transport of drugs in cell culture. I: A model for studying the passive diffusion of drugs over intestinal absorptive (Caco-2) cells. J Pharm Sci. 1990;79:476-482.

(29) Shu S, Zhang X, Wu Z, Wang Z, Li C. Delivery of protein drugs using nanoparticles self-assembled from dextran sulphate and quaternized chitosan. J Control Release. 2011;152:170-172.

(30) Leonard M, Fournier C, Dellacherie E. Comparative pore structure analysis of dextran-coated polystyrene particles. J Colloid Interface Sci. 1999;220:380-386.

(31) Houga C, Le Meins JF, Borsali R, Taton D, Gnanou Y. Synthesis of ATRP-induced dextran-b-polystyrene diblock copolymers and preliminary investigation of their self-assembly in water. Chem Commun. 2007;29:3063-3065.

(32) Ramirez JC, Sanchez-Chaves M, Arranz F. Functionalization of dextran with chloroacetate groups: immobilization of bioactive carboxylic acids. Polym. 1994;35:2651-2655.

(33) Vollmer A, Voiges K, Bork C, Fiege K, Cuber K, Mischnick P. Comprehensive analysis of the substitution pattern in dextran ethers with respect to the reaction conditions. Anal Bioanal Chem. 2009;395:1749-1768.

(34) Sanchez-Chaves M, Arranz F. Synthesis of amidoxime-containing modified dextran. Polym. 1996;37:4403-4407.

(35) De Belder AN. Dextran. Amershaw Bioscience 2003; Report No:18-1166-12.

(36) Choi KC, Bang JY, Kim C, Kim PI, Lee SR, Chung WT, Park WD, Park JS, Lee YS, Song CE, Lee HY. Antitumor effect of adriamycin-encapsulated nanoparticles of poly(DL-lactide-co-glycolide)-grafted dextran. J Pharm Sci. 2009;98:2104-2112.

(37) Kulkarni SA, Feng S-. Effects of particle size and surface modification on cellular uptake and biodistribution of polymeric nanoparticles for drug delivery. Pharm Res. 2013;30(10):2512-22.

(38) Qi J, Yao P, He F, Yu C, Huang C. Nanoparticles with dextran/chitosan shell and BSA/chitosan core - Doxorubicin loading and delivery. Int J Pharm. 2010;393:176-184.

(39) Clancy AA, Gregoriou Y, Yaehne K, Cramb DT. Measuring properties of nanoparticles in embryonic blood vessels: Towards a physicochemical basis for nanotoxicity. Chem Phys Lett. 2010;488:99-111.

(40) Le Broc-Ryckewaert D, Carpentier R, Lipka E, Daher S, Vaccher C, Betbeder D, Furman C. Development of innovative paclitaxel-loaded small PLGA nanoparticles: Study of their

antiproliferative activity and their molecular interactions on prostatic cancer cells. Int J Pharm. 2013;454(2):712-719.

(41) Lien CF, Molnár E, Toman P, Tsibouklis J, Pilkington GJ, Górecki DC, Barbu E. In vitro assessment of alkylglyceryl-functionalized chitosan nanoparticles as permeating vectors for the blood-brain barrier. Biomacromolecules. 2012;13:1067-1073.

(42) Ragnaill MN, Brown M, Ye D, Bramini M, Callanan S, Lynch I, Dawson KA. Internal benchmarking of a human blood-brain barrier cell model for screening of nanoparticle uptake and transcytosis. Eur J Pharm Biopharm. 2011;77:360-367.

(43) Avdeef A. How well can in vitro brain microcapillary endothelial cell models predict rodent in vivo blood–brain barrier permeability? Eur J Pharm Sci. 2011;43:109-124.

(44) Deli MA, Abrahám CS, Kataoka Y, Niwa M. Permeability studies on in vitro blood-brain barrier models: physiology, pathology, and pharmacology. Cell Mol Neurobiol. 2005;25:59-127.

(45) Barar J, Omidi Y. Bioelectrical and permeability properties of brain microvasculature endothelial cells: effects of tight junction modulators. J Biol Sci. 2008;8:556-562.

(46) Ordahl CP, Williams BA, Denetclaw W. Determination and morphogenesis in myogenic progenitor cells: an experimental embryological approach. Curr Top Dev Biol. 2000;48:319-367.

Figure(1)

Click here to download high resolution image

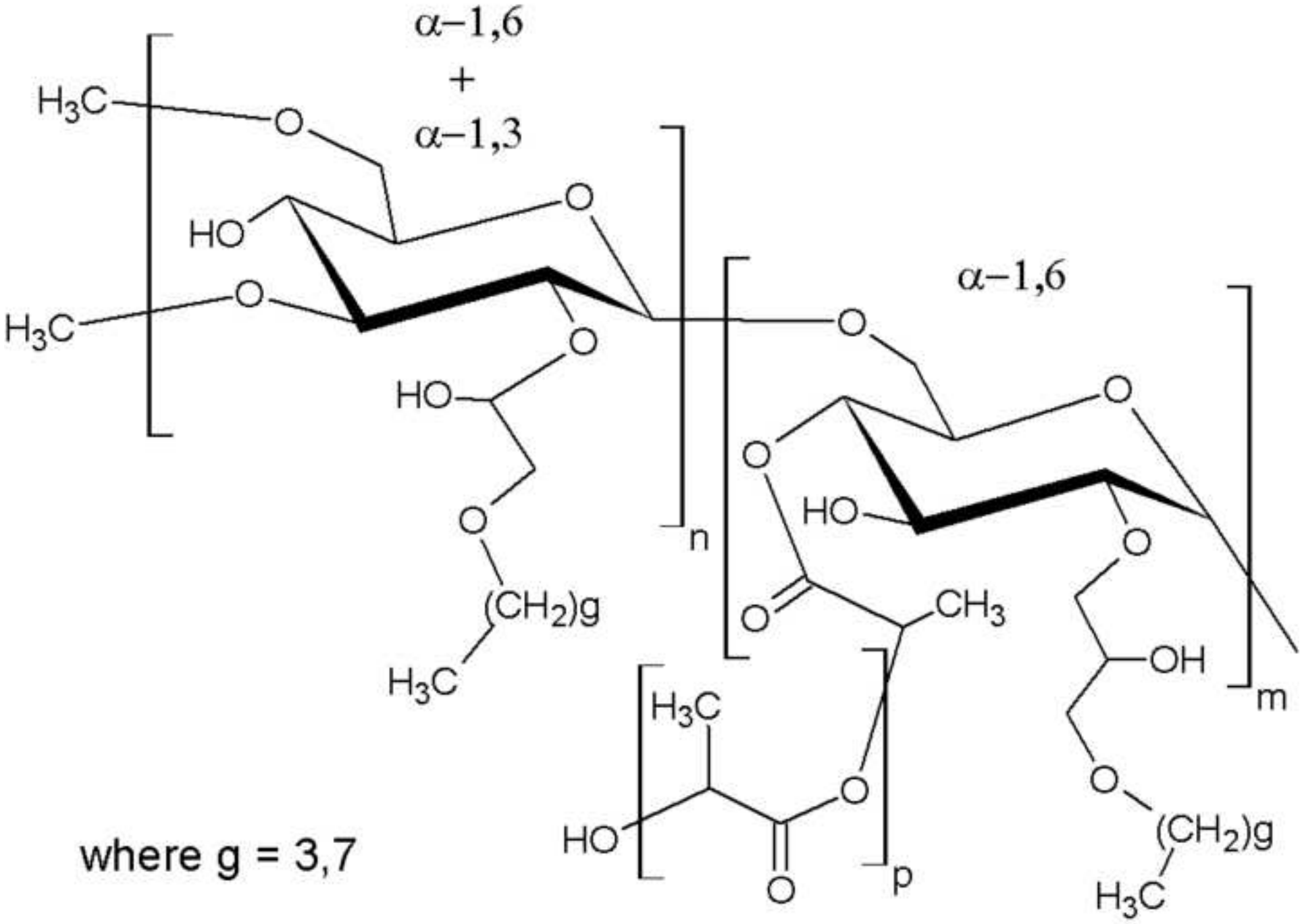

Figure(2)
Click here to download high resolution image

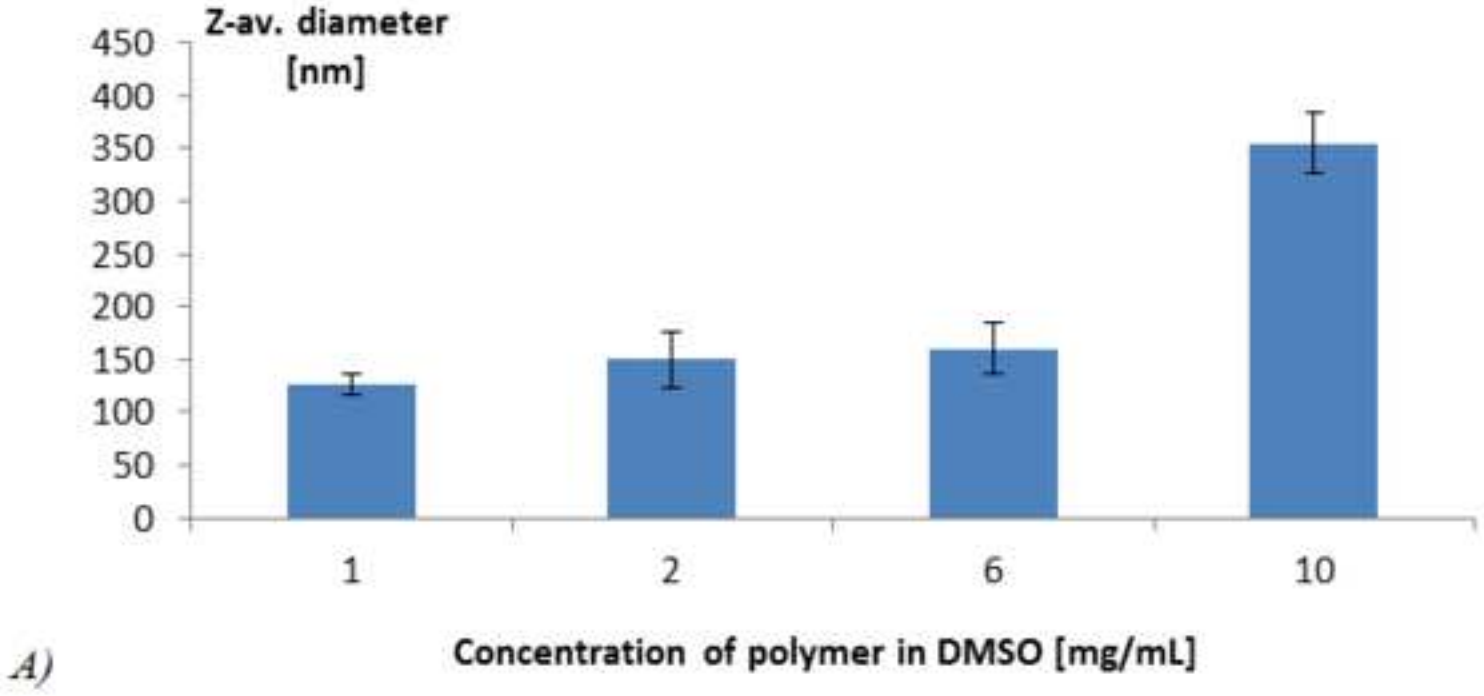

A)

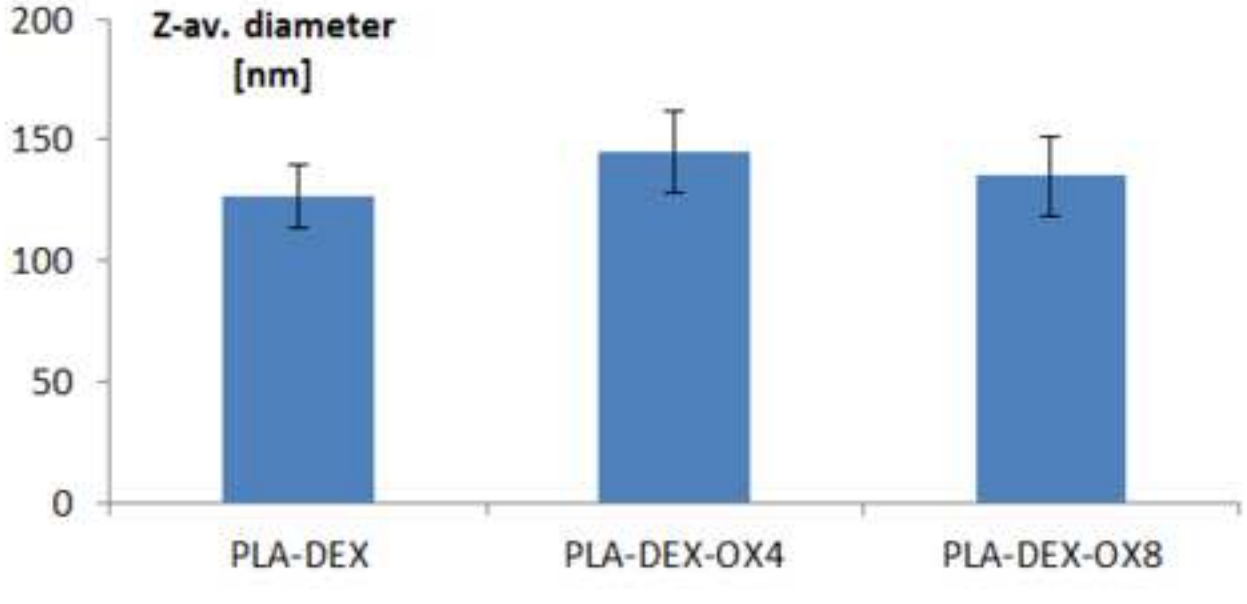

B)

Figure(3)
Click here to download high resolution image

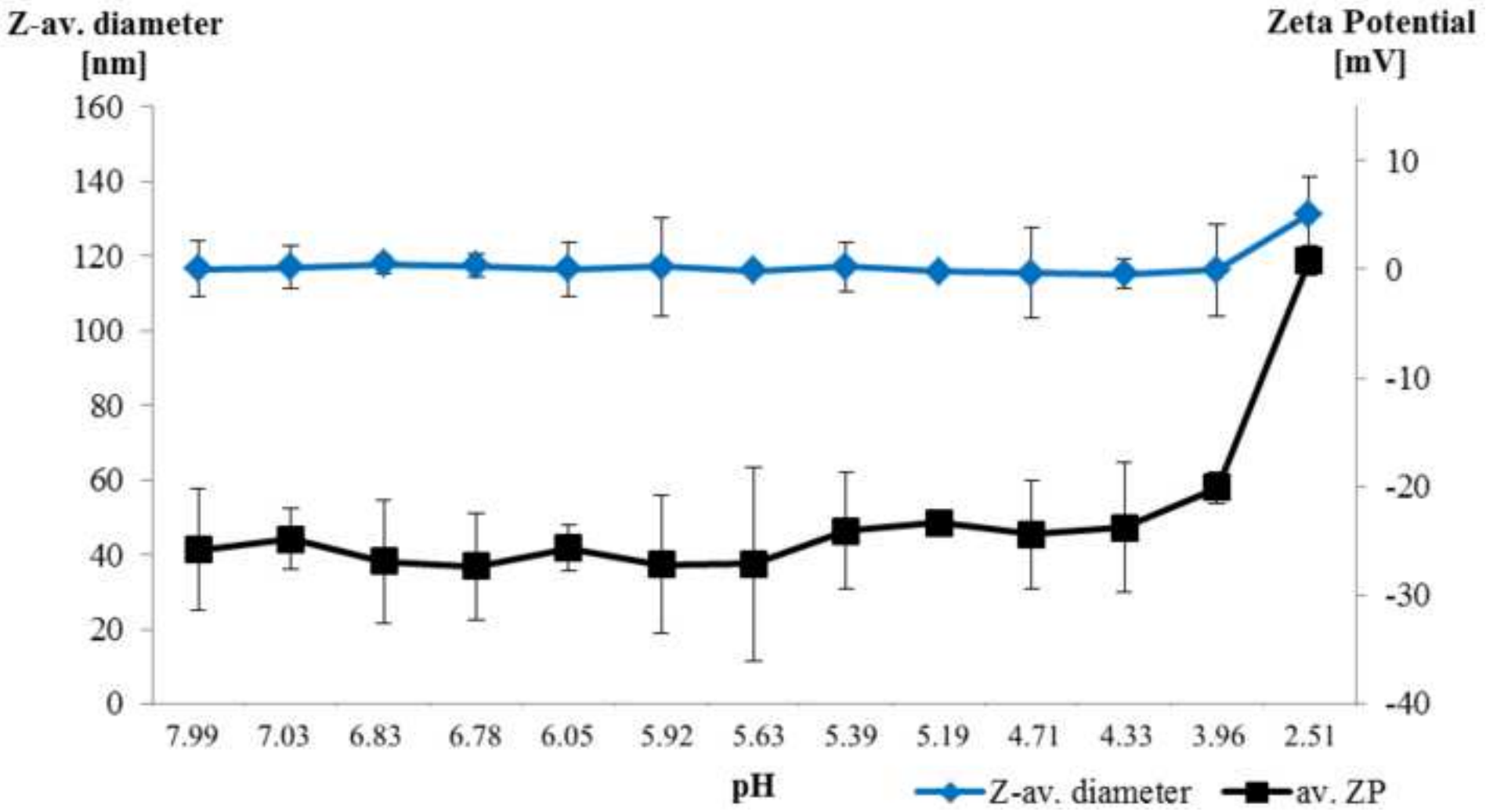

Figure(4)

Click here to download high resolution image

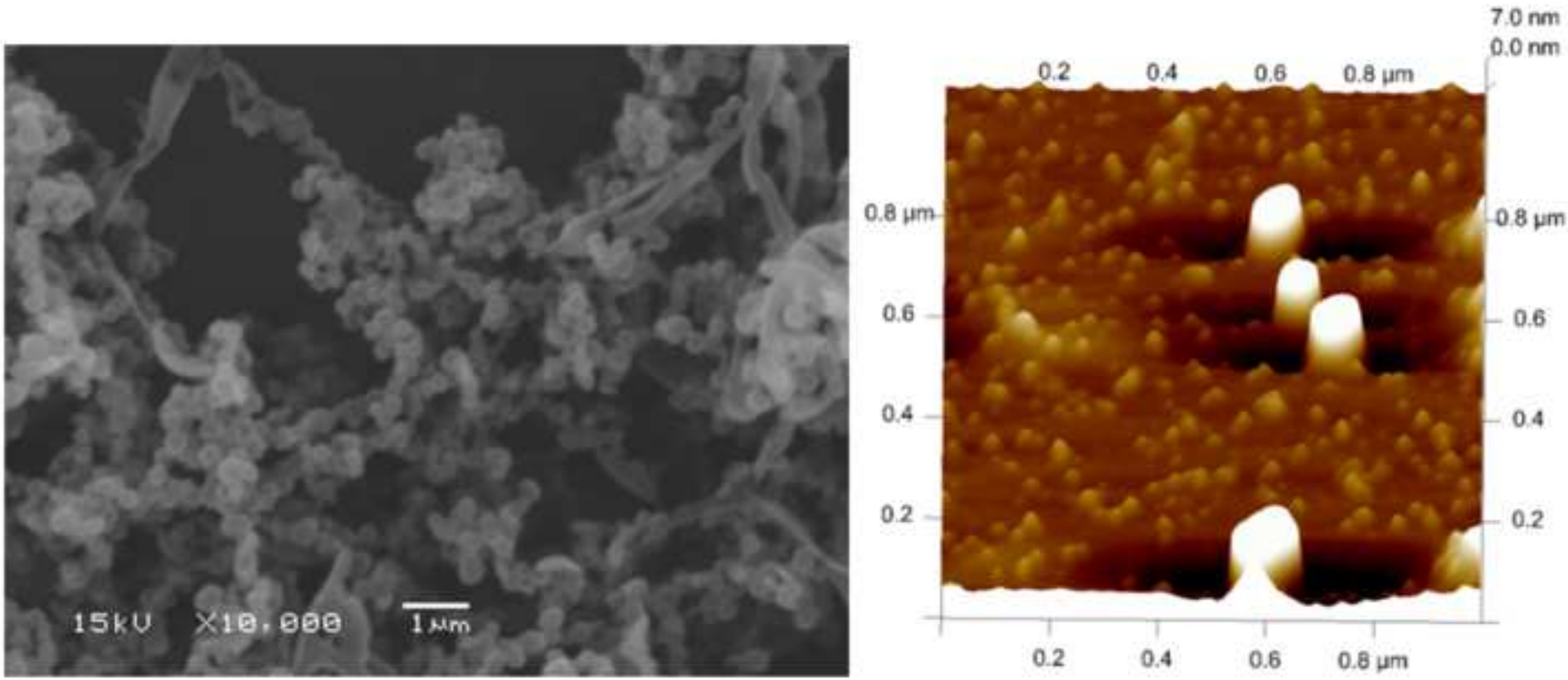

Figure(5)
Click here to download high resolution image

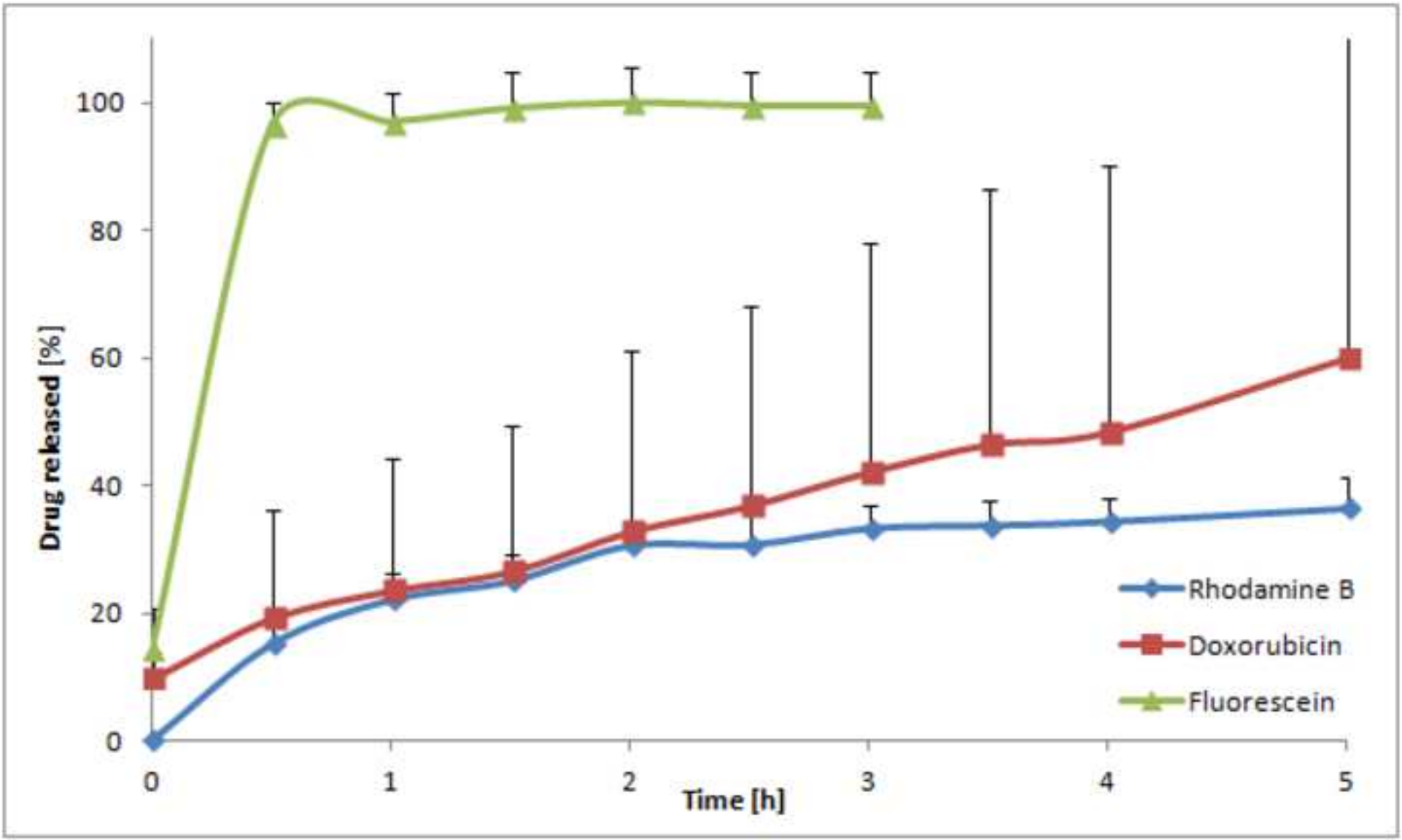

Figure(6)
Click here to download high resolution image

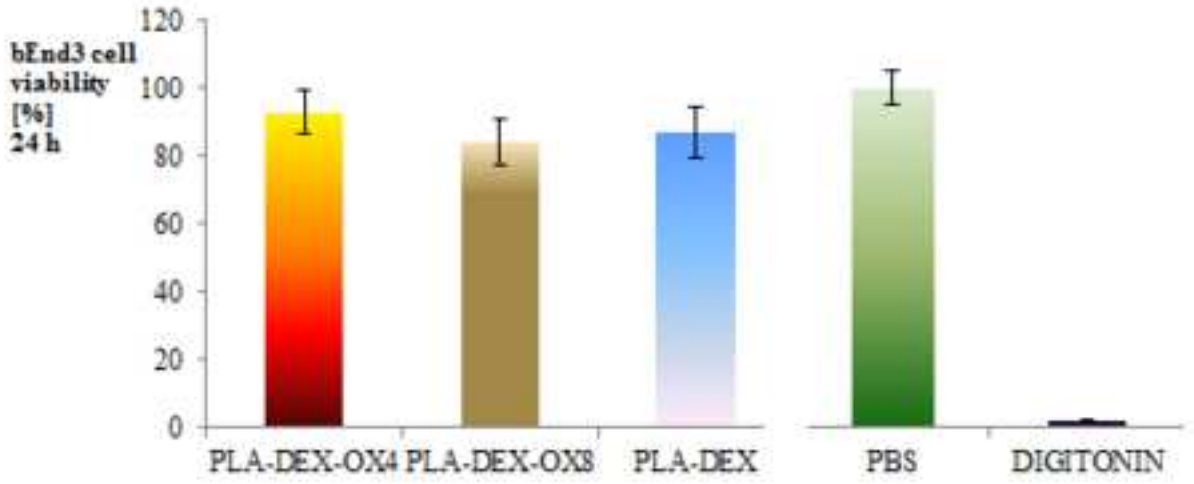

A)

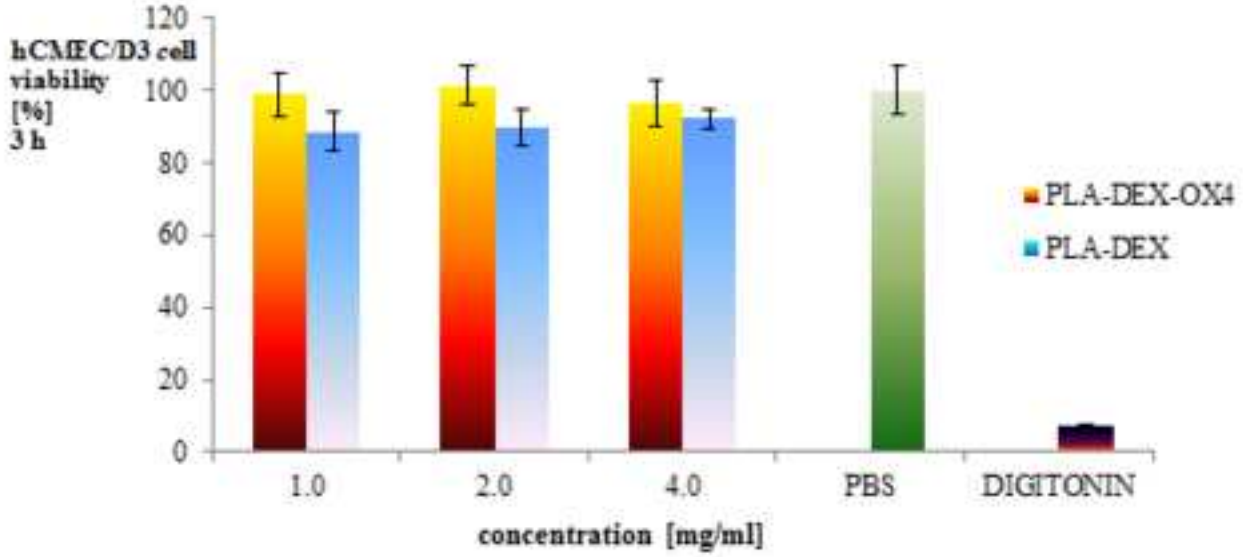

B)

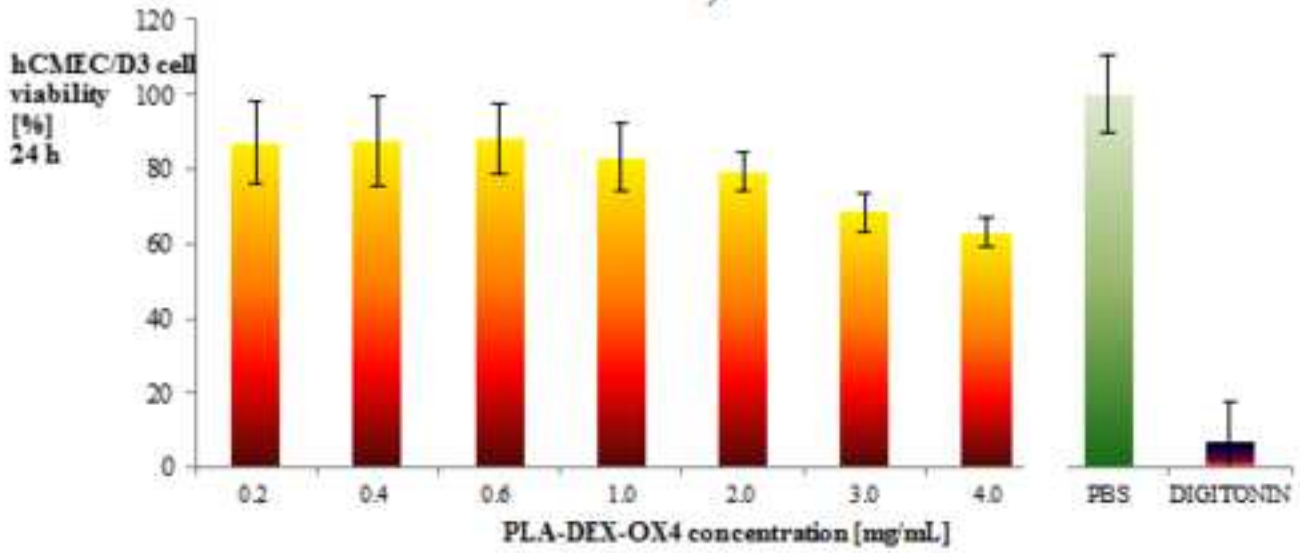

C)

Figure(7)
Click here to download high resolution image

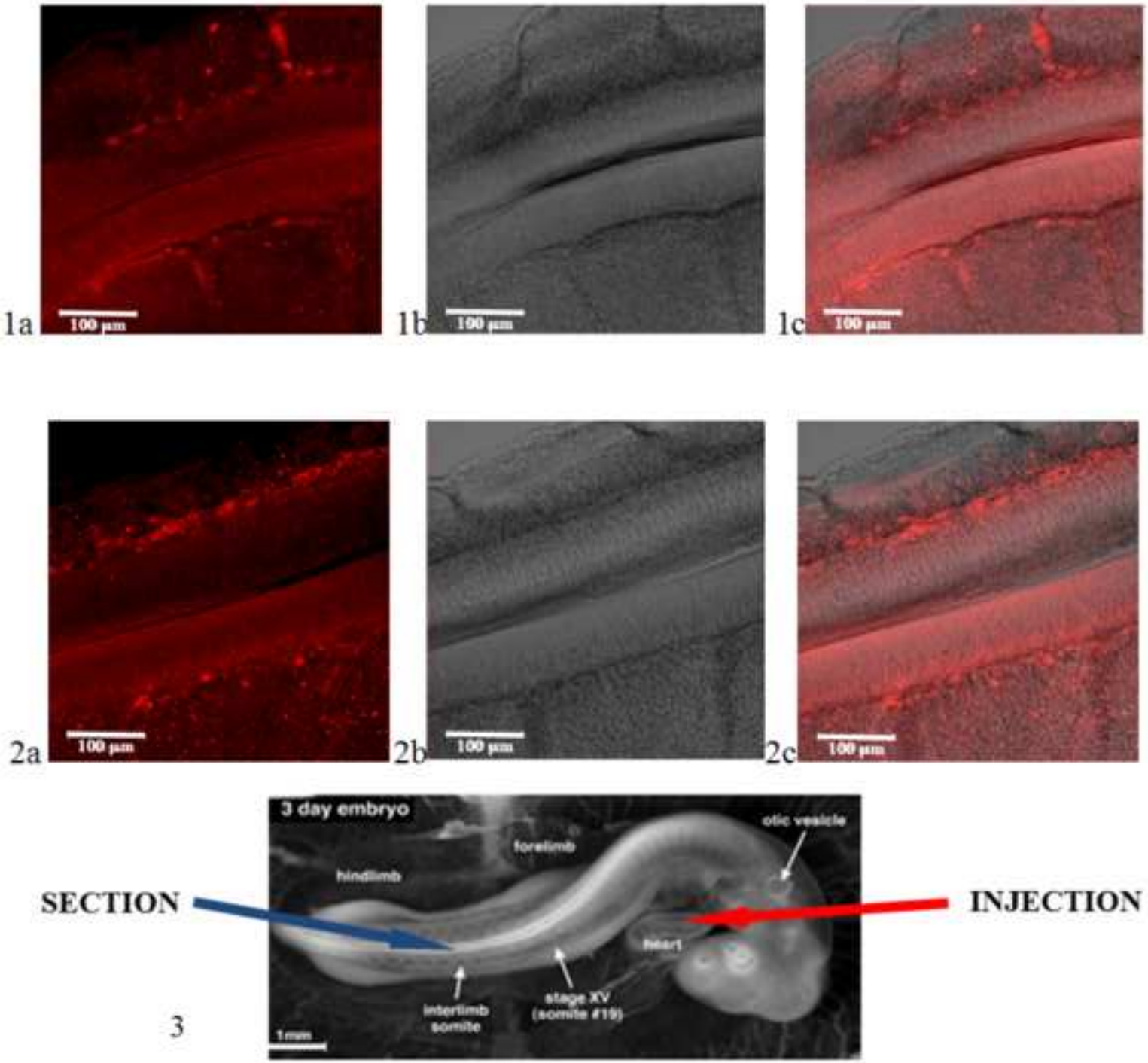

Figure(8)

Click here to download high resolution image

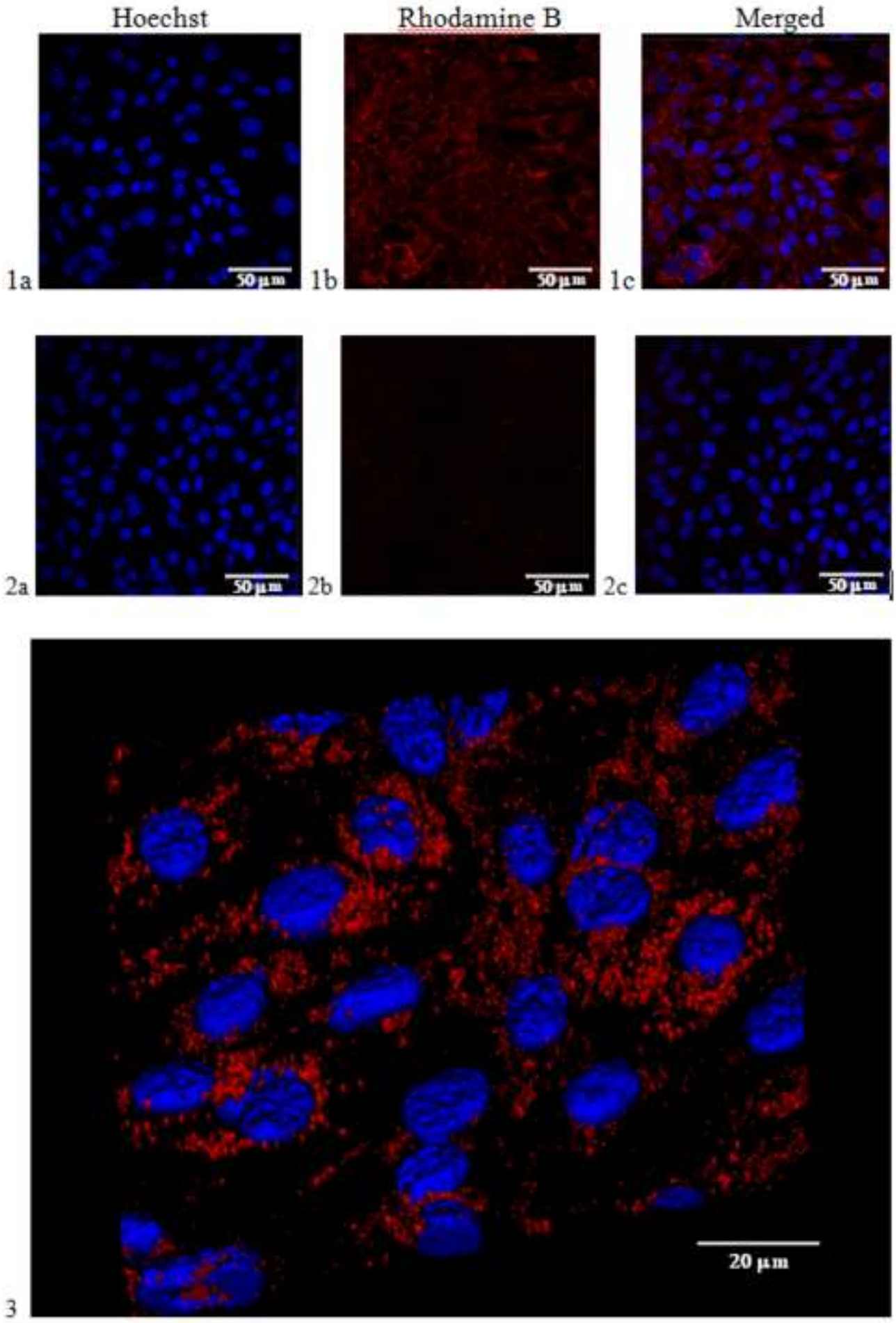

Figure(9)
Click here to download high resolution image

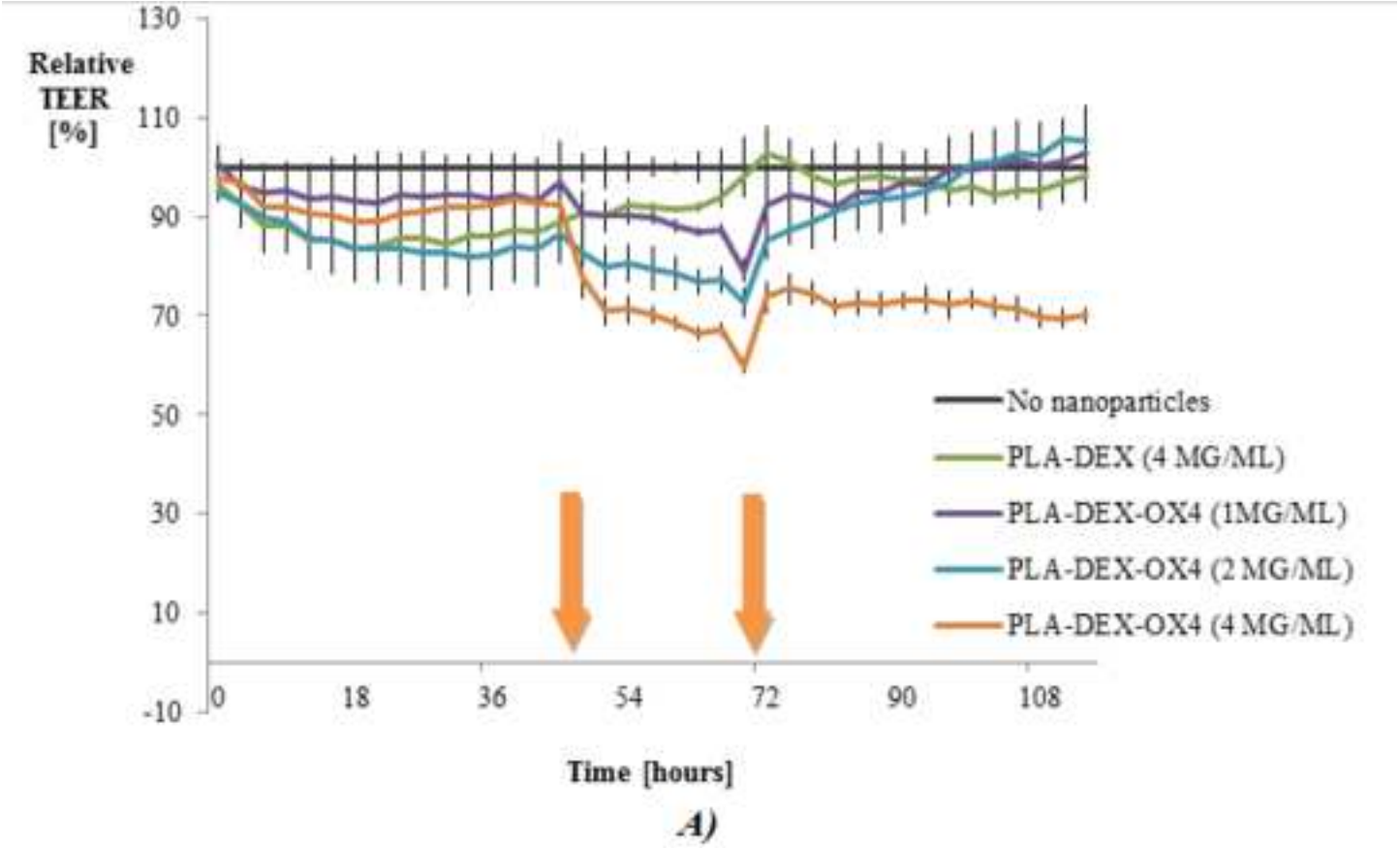

A)

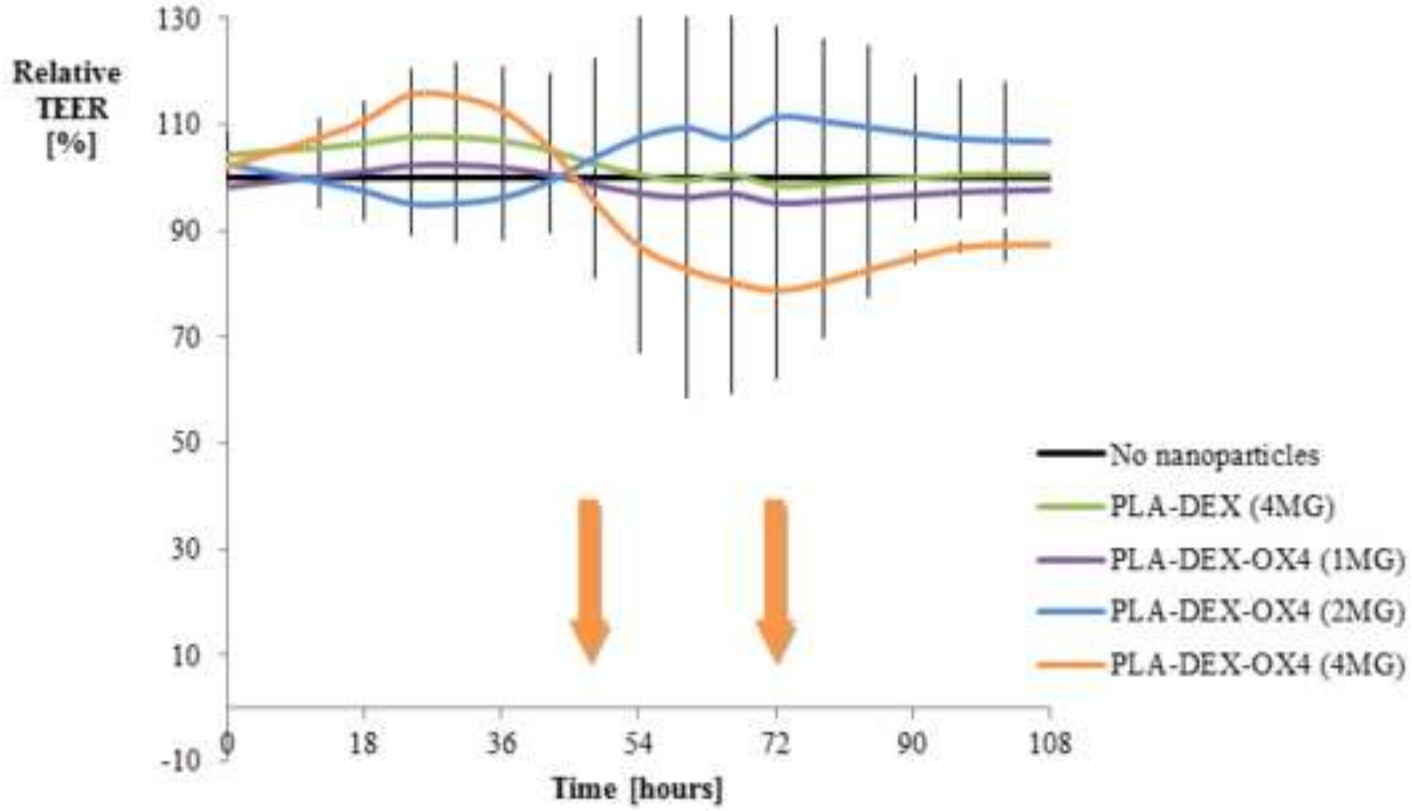

B)

Figure(10)

Click here to download high resolution image

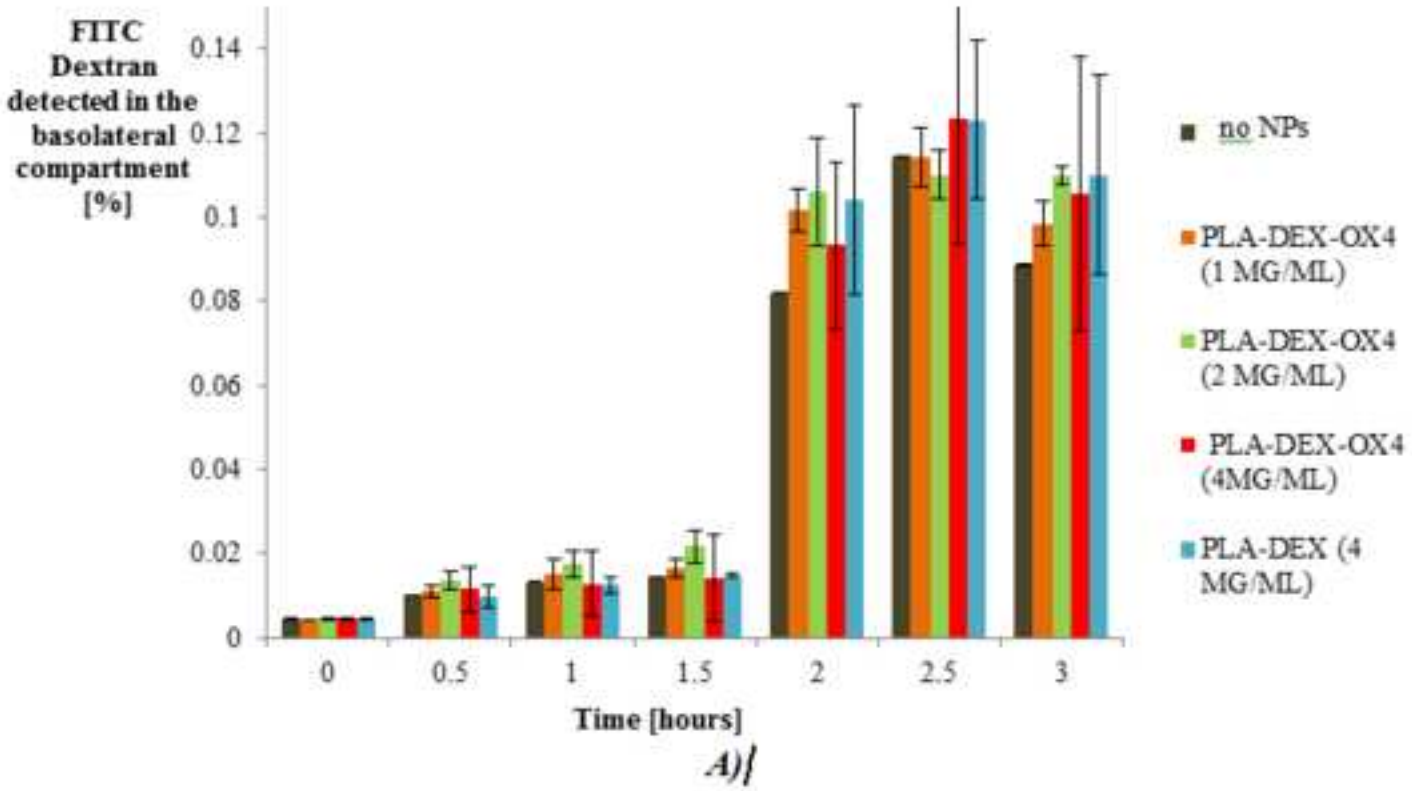

A)

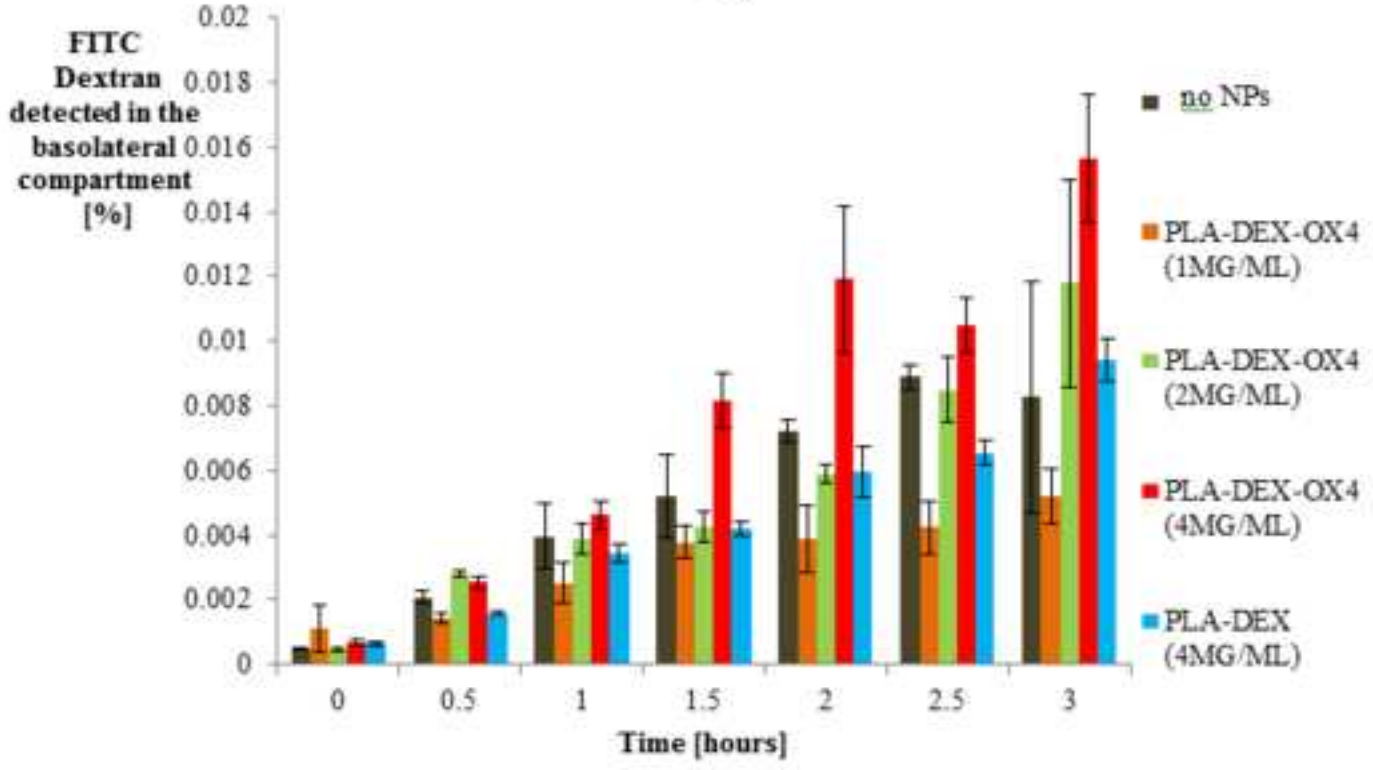

B)

Supplementary material

Click here to download Supplementary Material: supplementary material.docx

***Graphical Abstract**